Development/Plasticity/Repair

Suppressing CSPG/LAR/PTPσ Axis Facilitates Neuronal Replacement and Synaptogenesis by Human Neural Precursor Grafts and Improves Recovery after Spinal Cord Injury

Seyed Mojtaba Hosseini,[1] Arsalan Alizadeh,[1] Narjes Shahsavani,[1] Jeremy Chopek,[1] Jan-Eric Ahlfors,[2] and Soheila Karimi-Abdolrezaee[1,3]

[1]Department of Physiology and Pathophysiology, Spinal Cord Research Centre, Rady Faculty of Health Sciences, University of Manitoba, Winnipeg, Manitoba R3E0J9, Canada, [2]New World Laboratories, Laval, Quebec H7V 4A7, Canada, and [3]Children Hospital Research Institute of Manitoba, Winnipeg, Manitoba R3E3P4, Canada

Traumatic spinal cord injury (SCI) is a leading cause of permanent neurologic disabilities in young adults. Functional impairments after SCI are substantially attributed to the progressive neurodegeneration. However, regeneration of spinal-specific neurons and circuit re-assembly remain challenging in the dysregulated milieu of SCI because of impaired neurogenesis and neuronal maturation by neural precursor cells (NPCs) spontaneously or in cell-based strategies. The extrinsic mechanisms that regulate neuronal differentiation and synaptogenesis in SCI are poorly understood. Here, we perform extensive *in vitro* and *in vivo* studies to unravel that SCI-induced upregulation of matrix chondroitin sulfate proteoglycans (CSPGs) impedes neurogenesis of NPCs through co-activation of two receptor protein tyrosine phosphatases, LAR and PTPσ. In adult female rats with SCI, systemic co-inhibition of LAR and PTPσ promotes regeneration of motoneurons and spinal interneurons by engrafted human directly reprogramed caudalized NPCs (drNPC-O2) and fosters their morphologic maturity and synaptic connectivity within the host neural network that culminate in improved recovery of locomotion and sensorimotor integration. Our transcriptomic analysis of engrafted human NPCs in the injured spinal cord confirmed that inhibition of CSPG receptors activates a comprehensive program of gene expression in NPCs that can support neuronal differentiation, maturation, morphologic complexity, signal transmission, synaptic plasticity, and behavioral improvement after SCI. We uncovered that CSPG/LAR/PTPσ axis suppresses neuronal differentiation in part by blocking Wnt/β-Catenin pathway. Taken together, we provide the first evidence that CSPGs/LAR/PTPσ axis restricts neurogenesis and synaptic integration of new neurons in NPC cellular therapies for SCI. We propose targeting LAR and PTPσ receptors offers a promising clinically-feasible adjunct treatment to optimize the efficacy and neurologic benefits of ongoing NPC-based clinical trials for SCI.

Key words: **human neural precursor cells; neurogenesis; neurological recovery; spinal cord injury; synaptogenesis; transplantation**

Significance Statement

Transplantation of neural precursor cells (NPCs) is a promising approach for replacing damaged neurons after spinal cord injury (SCI). However, survival, neuronal differentiation, and synaptic connectivity of transplanted NPCs within remain challenging in SCI. Here, we unravel that activation of chondroitin sulfate proteoglycan (CSPG)/LAR/PTPσ axis after SCI impedes the capacity of transplanted human NPCs for replacing functionally integrated neurons. Co-blockade of LAR and PTPσ is sufficient to promote re-generation of motoneurons and spinal V1 and V3 interneurons by engrafted human caudalized directly reprogramed NPCs (drNPC-O2) and facilitate their synaptic integration within the injured spinal cord. CSPG/LAR/PTPσ axis appears to suppress neuronal differentiation of NPCs by inhibiting Wnt/β-Catenin pathway. These findings identify targeting CSPG/LAR/PTPσ axis as a promising strategy for optimizing neuronal replacement, synaptic re-connectivity, and neurologic recovery in NPC-based strategies.

Received Nov. 1, 2021; revised Feb. 24, 2022; accepted Feb. 26, 2022.

Author contributions: S.M.H. and S.K.-A. designed research; S.M.H., A.A., N.S., J.C., and S.K.-A. performed research; J.-E.A. contributed unpublished reagents/analytic tools; S.M.H., A.A., and J.C. analyzed data; S.M.H. wrote the first draft of the paper; S.K.-A. edited the paper; S.K.-A. wrote the paper.

This work was supported by Canadian Institutes of Health Research (CIHR) Grants 133721 and 156218 (to S.K.-A.). S.M.H. and N.S. had studentship support from University of Manitoba Graduate Fellowship, Will-to-Win/Manitoba Paraplegic Foundation, and the University of Manitoba GETS program.

J.E.A. is a shareholder of New World Laboratories Inc. All other authors declare no competing financial interests.

Correspondence should be addressed to Soheila Karimi-Abdolrezaee at soheila.karimi@umanitoba.ca.

https://doi.org/10.1523/JNEUROSCI.2177-21.2022

Introduction

Traumatic spinal cord injury (SCI) results in lifelong neurologic disabilities that are substantially attributed to the permanent degeneration of spinal neurons and loss of their synaptic connectivity (Fischer et al., 2020). Spontaneous neurogenesis is restricted after SCI because of the overall loss of resident neural precursor cells (NPCs) within the lesion, and predominant gliogenesis of surviving NPCs (Assinck et al., 2017; Shao et al., 2019; Zholudeva and Lane, 2019; Fischer et al., 2020). Accordingly, transplantation of exogenous adult multipotent NPCs has been pursued for cell replacement in SCI preclinical models owing to their innate multilineage potential to generate neurons and glia (Iwanami et al., 2005; Karimi-Abdolrezaee et al., 2006, 2010; Nori et al., 2015; Rosenzweig et al., 2018; Yu et al., 2019; Ahuja et al., 2020; Ceto et al., 2020). While these studies show the promise of transplanting NPCs for promoting oligodendrogenesis and white matter repair in SCI (Karimi-Abdolrezaee et al., 2006, 2010; Salewski et al., 2015; Sankavaram et al., 2019), to date limited success has been attained on neurogenesis (Deng et al., 2011; Khazaei et al., 2020; Yang et al., 2021). A major roadblock to efficient neuronal replacement in SCI is the limited extrinsic support for neuronal differentiation and an inhibitory extracellular milieu that impedes new neurons to mature into spinal-specific subtypes and make synaptic contacts. These challenges have also limited the neurologic benefits of NPC therapies in SCI clinical trials (Curtis et al., 2018; Jin et al., 2019; Levi et al., 2019). Hence, there are currently critical knowledge gaps in understanding the mechanisms regulating neurogenesis, maturation, and integration of transplanted NPCs after SCI. This knowledge enables development of new targeted therapies to facilitate regeneration of spinal cord-specific neurons and re-assembly of neural network within the injured spinal cord.

Upregulation of matrix chondroitin sulfate proteoglycans (CSPGs) significantly contributes to the dysregulated milieu of SCI lesion (Dyck and Karimi-Abdolrezaee, 2015; Hussein et al., 2020; Mukherjee et al., 2020). CSPGs are known for their inhibitory effects on axon regeneration and plasticity in SCI (McKeon et al., 1991; Barritt et al., 2006; Galtrey et al., 2007; Alilain et al., 2011; Lang et al., 2015). Our group identified that CSPGs also restrict self-renewal and survival of NPCs *in vitro* (Dyck et al., 2015, 2019), and *in vivo* degradation of CSPGs by chondroitinase ABC (ChABC) can improve long-term survival and mobilization of engrafted mouse NPCs in the injured spinal cord (Karimi-Abdolrezaee et al., 2010). At the molecular levels, our *in vitro* investigations uncovered that CSPGs can directly regulate proliferation and survival of NPCs by activating two protein tyrosine phosphatase receptors, LAR and PTPσ, which are highly expressed in NPCs (Dyck and Karimi-Abdolrezaee, 2015; Dyck et al., 2015). Interestingly, both LAR and PTPσ mediate the inhibitory effects of CSPGs of NPCs *in vitro*. In rat SCI, pharmacological inhibition of LAR and/or PTPσ acutely after injury has resulted in enhanced endogenous oligodendrogenesis (Dyck et al., 2019) and axon regeneration (Fisher et al., 2011; Lang et al., 2015; Cheng et al., 2021). However, the role and mechanisms of CSPG signaling in regulating neurogenesis and synaptogenesis of NPCs *in vitro* and after transplantation in SCI is currently unexplored.

In the current study, we sought to address: (1) whether CSPGs block neurogenesis and whether this effects is through LAR and/or PTPσ mediated mechanisms; (2) whether impairing LAR and PTPσ is sufficient to enhance long-term survival, mobilization and integration of NPCs after transplantation into the injured spinal cord; (3) whether targeting of LAR and PTPσ enhances differentiation of engrafted human derived NPCs into spinal-specific neurons; and (4) whether CSPGs impede synaptogenesis and targeting their receptors would facilitate synaptic connectivity of NPC-derived newborn neurons within the spinal cord network. We have employed human directly reprogramed caudalized NPCs (drNPC-O2) with the capacity to generate spinal motoneurons and interneurons. We have also used specific functional blocking peptides to impair LAR and PTPσ. We performed extensive *in vitro* and *in vivo* approaches to unravel that perturbing CSPG signaling promotes graft survival and neurogenesis of human drNPC-O2 and enhances physiological and structural maturation of new neurons and their synaptic connectivity that correlates with recovery of locomotion and sensorimotor integration in rats with SCI. RNA sequencing (RNA-seq) and *in vitro* validations identified that CSPG/LAR/PTPσ axis impedes neurogenesis of human NPCs, at least in part, by blocking Wnt/β-Catenin pathway. Taken together, we provide the first evidence that CSPGs through LAR and PTPσ signaling negatively control neuronal differentiation and synaptogenesis, and pharmacological inhibition of this axis provides a novel, promising target to promote functional replacement of spinal cord-specific neurons by human NPC grafts associated with neurologic recovery in severe SCI.

Materials and Methods

All functional and neuroanatomical assessments in this study were performed blindly with proper randomization. For tissue analysis, unbiased stereological approaches were used. Information on all antibodies and key reagents is provided in Table 1.

Animals

All animal studies were performed in compliance with the animal policies and approved protocols by the Animal Care Committee of the University of Manitoba according to the Canadian Council of Animal Care guidelines. For *in vivo* studies, a total of 50 adult female Sprague Dawley (SD) rats (250–300 g) were used. Animals were housed in standard plastic cages in a 12/12 h light/dark cycle before SCI and afterward in cages covered with soft bedding to prevent skin erosions and urine scalding. Animals had free access to food and drinking water.

Human caudalized directly reprogramed NPCs (drNPC-O2)

Human caudalized drNPC-O2 (drNPC-O2) were provided by New World Laboratories (NWL). The cells were cultured with drNPC-O2 growth media which contains DMEM/F12 (50 ml, catalog #11330032, Invitrogen), Neurobasal (50 ml, catalog #A13712-01, Invitrogen), CD lipid (0.1 ml, catalog #A13712-01, Invitrogen), Glutamax (0.5 ml, catalog #A12860-01, Invitrogen), drNPCs-O2 supplement (1.45 ml, catalog #O2-cell-01, NWL), and Growth Factor-drNPC-O2 supplement (80 µl, catalog #O2-supp-01, NWL).

Immunocytochemistry for *in vitro* assessments

For immunocytochemistry in all assessments, cells were fixed with 3% paraformaldehyde (PFA) for 20 min at room temperature. Next, cells were blocked (5% skim milk, 0.3% Triton X-100 in 0.1 M PBS) for 1 h at room temperature. After blocking, cells were incubated with primary antibodies overnight at 4°C (Table 1) followed by incubation for 1 h with proper secondary antibodies (Table 1). For double immunostaining, cells were incubated with the second primary antibody and secondary antibody. Between each step, cells were washed three times with 0.1 M PBS. Lastly, all cells nuclei were stained with 4′,6′-diamidino-2-phenylindole (DAPI; 1:1000) for 20–30 min at room temperature (Alizadeh et al., 2017; Hart et al., 2020).

Table 1. List of antibodies that were used for immunostaining and protein analysis

Antibody	Host	Application	Dilution factor	Company (catalog #)
Nestin	Mouse	ICC	1:50	DSHB (Rat-401-s)
LAR	Rabbit	ICC	1:50	Santa Cruz (sc-25434)
PTPσ	Goat	ICC	1:100	Santa Cruz (sc-10871)
OTX-2	Mouse	ICC	1:50	DSHB (PCRP-OTX2-1E10)
CDX-2	Mouse	ICC	1:50	DSHB (PCRP-CDX2-1A3)
HOXB-2	Mouse	ICC	1:50	DSHB (PCRP-HOXB2-1F2)
HOXB-6	Mouse	ICC	1:50	DSHB (PCRP-1A4)
β-Tubulin-III	Mouse	ICC	1:600	Sigma (T8660)
	Chicken	ICC		Abcam (41489)
GFAP	Rabbit	ICC	1:1000	Dako (Z0334)
GFAP	Mouse	IHC	1:800	Sigma (G3893)
O4	Mouse	ICC	1:300	R&D Systems (MAB1326)
ChAT	Rabbit	ICC, IHC	1:250	Millipore (AB143)
EVX.1	Mouse	ICC, IHC	1:50	DSHB (99.1-3A2)
LHX-2	Mouse	ICC, IHC	1:50	DSHB (PCRP-LHX2-3B11)
En.1	Rabbit	ICC, IHC	1:500	Millipore (AB5732)
SCL	Mouse	ICC, IHC	1:50	DSHB (PCRP-SCXA-1D2)
SIM.1	Rabbit	ICC	1:500	Thermo Fisher (PAS-40693)
		IHC	1:200	
Anti-BrdU	Mouse	ICC	1:500	BD Bioscience (555627)
Synaptophysin	Mouse	ICC	1:5000	Millipore (MAB329)
Synaptophysin	Rabbit	IHC	1:200	Alomone (ANR-013)
PSD95	Rabbit	ICC	1:250	Alomone (APZ009)
Nav	Mouse	ICC	1:1000	Sigma (S8809)
Kv2.1	Rabbit	ICC	1:250	Alomone (APC-012)
MAP-2	Mouse	ICC	1:500	Millipore (MAB3418)
GluA1	Guinea pig	ICC	1:250	Alomone (AGP-009)
STEM121	Mouse	IHC	1:500	Takara (Y40410)
HNA	Mouse	IHC	1:500	Millipore (MAB1281)
Olig2	Rabbit	IHC	1:1000	Millipore (AB9610)
Ku80	Rabbit	IHC	1:500	Cell Signaling (2753)
NeuN	Mouse	IHC	1:150	Chemicon (MAB377)
vGlut1	Guinea pig	IHC	1:250	Millipore (AB5905)
GABAr	Guinea pig	IHC	1:250	Alomone (AGP-083)
Alexa Flour 488-goat anti-mouse	Goat	ICC	1:750	Invitrogen (A11029)
		IHC	1:600	
Alexa Flour 568-goat anti-mouse	Goat	ICC	1:750	Invitrogen (A11031)
		IHC	1:600	
Alexa Flour 488-goat anti-rabbit	Goat	ICC	1:750	Invitrogen (A11034)
		IHC	1:600	
Alexa Flour 568-goat anti-rabbit	Goat	ICC	1:750	Invitrogen (A11036)
		IHC	1:600	
Alexa Flour 647-goat anti-mouse	Goat	IHC	1:600	Invitrogen (A21236)
Alexa Flour 647-goat anti-rabbit	Goat	IHC	1:600	Invitrogen (A21245)
Alexa Flour 568-goat anti-guinea pig	Goat	ICC	1:750	Sigma (AP193C)
		IHC	1:600	
Anti-HRP	Mouse	SB	1:4000	Sigma (A0168)

Culture, characterization, and differentiation of human caudalized NPCs on laminin and CSPGs substrate

To prepare laminin and CSPG substrates for plating human caudalized drNPC-O2, culture dishes were first coated with poly-L-lysine (PLL; 100 μg/ml, catalog #P6282, Sigma-Aldrich) overnight at room temperature followed by laminin (5 μg/ml, catalog #L2020, Sigma-Aldrich) with or without CSPGs mixture (5 μg/ml, catalog #CC117, Sigma-Aldrich) for 6 h at 37°C. CSPGs mixture contained neurocan, phosphacan, versican, and aggrecan, the major variants present in SCI milieu. Then, drNPC-O2 were plated at 15,000 cells/cm^2 onto laminin or laminin+CSPGs substrate in drNPC-O2 growth media containing DMEM/F12 (50 ml, catalog #11330032, Invitrogen), Neurobasal (50 ml, catalog #A13712-01, Invitrogen), CD lipid (0.1 ml, catalog #A13712-01, Invitrogen), Glutamax (0.5 ml, catalog #A12860-01, Invitrogen), drNPCs-O2 supplement (1.45 ml, catalog #O2-cell-01, NWL), and Growth Factor-drNPC-O2 supplement (80 μl, catalog #O2-supp-01, NWL). To verify multipotent properties of drNPC-O2, cells in growth media were fixed at 6 h postseeding with 3% PFA and immunostained with Nestin antibody. For assessments of cell attachment, proliferation and survival, drNPC-O2 were maintained in growth media for 2 d. For differentiation assessment, cells were maintained in drNPC-O2 differentiation media containing DMEM/F12 (50 ml, catalog #11330032, Invitrogen), Neurobasal (50 ml, catalog #A13712-01, Invitrogen), CD lipid (0.1 ml, catalog #A13712-01, Invitrogen), Glutamax (0.5 ml, catalog #A12860-01, Invitrogen), drNPCs-O2 supplement (1.45 ml, catalog #O2-cell-01, NWL), and T3-drNPC-O2 supplement (67 ml, catalog #O2-supp-02, NWL) for two weeks and half of the media was refreshed twice a week. Then, cells were fixed with PFA and immunostained for tri-neural lineage markers: β-tubulin-III antibody (β-tubulin-III, neurons), O4 (oligodendrocytes), and GFAP (astrocytes). To further characterize neuronal subtypes, differentiated drNPC-O2 were immunostained with antibodies against ChAT (motoneuron marker), EVX.1 (dl1 spinal interneuron), LHX-2 (dl2 and dl4 spinal interneurons), EN.1 (V1 spinal interneuron), SCL (V2 spinal interneuron), and SIM.1 (V3 spinal interneuron). Summary of *in vitro* experimental design is provided in Figure 1*A*.

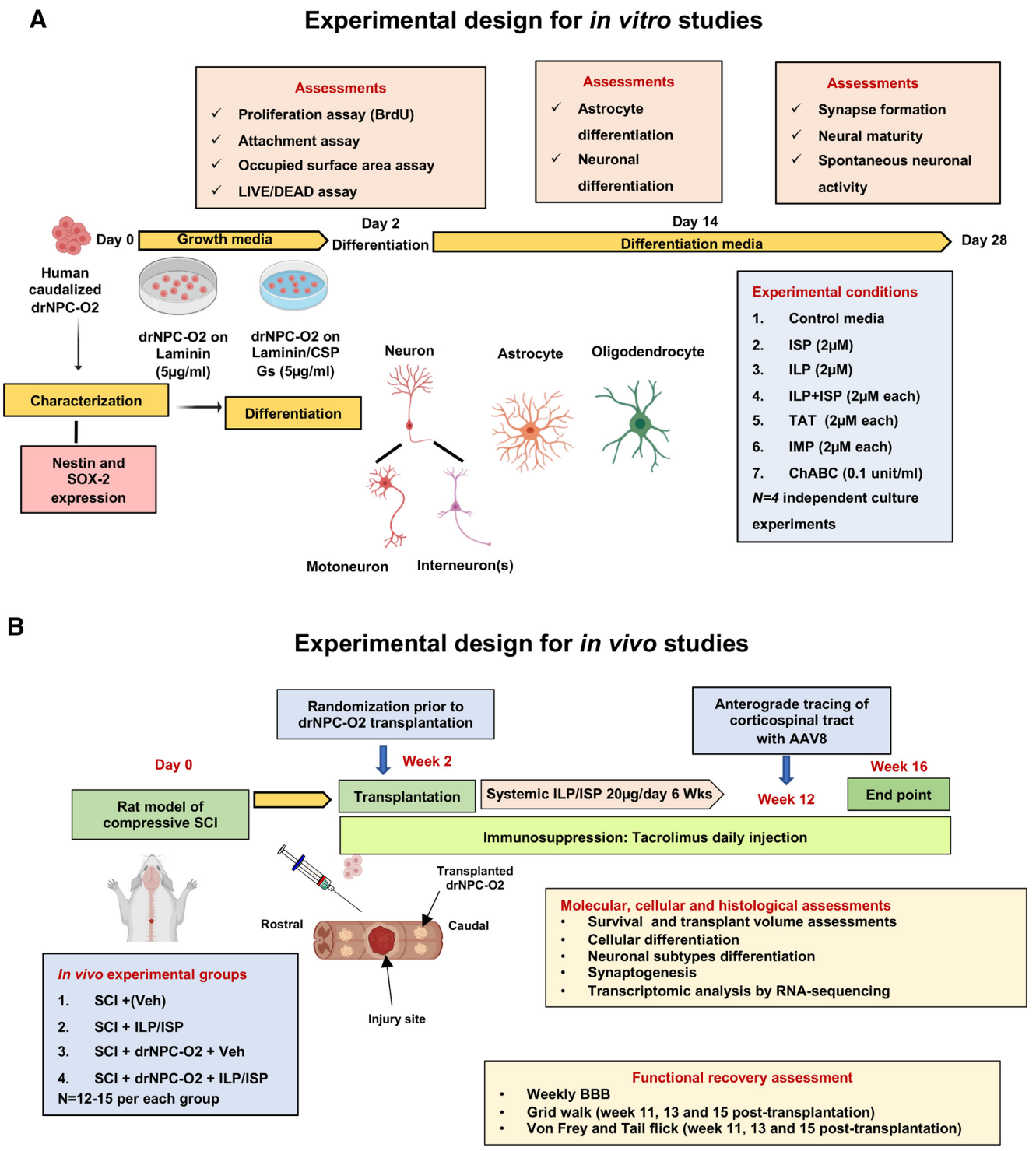

Figure 1. Schematic diagram of experimental design and timelines for *in vitro* (***A***) and animal studies (***B***).

***In vitro* assessments of ILP and ISP peptides in blocking LAR and PTPσ mediated effects of CSPGs on drNPC-O2**

We blocked LAR and PTPσ receptors by two specific inhibitory peptides; ILP (NH2-GRKKRRQRRRCDLADNIERLKANDGLKFSQEYESI-NH2) and ISP (NH2-GRKKRRQRRRCDMAEHMERLKANDSLKLSQE YESI-NH2), respectively, as we described previously (Dyck et al., 2015, 2019; Lang et al., 2015). To determine an efficient concentration of ILP and ISP in blocking LAR and PTPσ receptors in human drNPC-O2, we performed an *in vitro* concentration gradient assay by examining survival, attachment and cell spreading of drNPC-O2 on laminin or laminin+CSPGs substrate (assessments are described below). Cells were plated on laminin and laminin+CSPGs and treated with ILP and/or ISP at concentrations of 1, 2, 5, 8, and 10 μM. These assessments indicated that ILP and/or ISP at 2 μM was the most efficient concentration to significantly block CSPG inhibitory effects on drNPC-O2. To confirm the specificity of ILP and ISP, we employed a control peptide, intracellular Mu peptide (IMP; NH2-LLQHITQMKCAEGYGFKEEYESGRKKRRQ RRRC-NH2), designed to block PTPσ, another member of the PTP receptor family (Xie et al., 2006). Since all peptides contained a TAT (transcription of human immunodeficiency) domain (GRKKRRQRRRC) to facilitate intracellular delivery, we also included TAT as another control peptide to rule out any possible effect on drNPC-O2. To verify the

specificity of CSPG effects per se, we also used ChABC (0.1 U/ml), a CSPGs degrading enzyme (catalog #C3667-10UN, Sigma-Aldrich) and ROCK inhibitor (Y-27632, 10 μM, catalog #73804, StemCell Technologies) as we described previously (Dyck et al., 2015, 2019).

Assessment of cell attachment and spreading of drNPC-O2 in vitro

We functionally assessed the capacity of drNPC-O2 to attach and spread on laminin or laminin+CSPGs substrate (Dyck et al., 2015, 2019). In each assessment, experimental conditions were as follows: (1) control; (2) ILP; (3) ISP; (4) ILP+ISP; (5) TAT; (6) IMP; (7) ChABC; and (8) ROCK inhibitor. Two days in culture, drNPC-O2 were fixed with 3% PFA and stained with DAPI (1:10,000, catalog #D8417, Sigma-Aldrich) as a nuclear marker. Cellular attachment and the spreading area were measured as we previously described (Dyck et al., 2015, 2019). Briefly, we unbiasedly measured the total occupied area of drNPC-O2 using StereoInvestigator Cavalieri probe (MBF Bioscience) in 8–10 separate bright-field images under 20× objective containing an average of 300 cells per experimental condition. The occupied surface area was normalized to the total number of DAPI+ cells to calculate area per cell (Dyck et al., 2015, 2019).

Assessment of drNPC survival, proliferation, and differentiation in vitro

For survival and proliferation assays, drNPC-O2 (15,000 cells/cm^2) were plated onto laminin or laminin+CSPGs substrate for 2 d. Cell viability was assessed using the LIVE/DEAD kit according to the manufacturer instructions (LIVE/DEAD Viability/Cytotoxicity kit; catalog #L3224, Thermo Fisher Scientific). For cellular quantification, 8–10 images were randomly captured under 20× objective for Calcein (494 nm, live cells) and EthD-1 (528 nm, dead cells) containing an average of 300 cells per experimental condition. The percentage of live cells was calculated by dividing the total number of live cells (green) to the total number of live and dead cells in analyzed fields in each condition.

For cell proliferation, 2 d after plating, drNPC-O2 were treated with bromodeoxyuridine (BrdU; 20 μM, catalog #B5002, Sigma-Aldrich) for 3 h at 37°C, and then fixed with 3% PFA and incubated in 2 N HCl and 0.5% Triton X-100 for 30 min at 37°C. Next, they were washed with 0.1 M sodium borate in PBS for 10 min, incubated with anti-BrdU antibody overnight at 4°C and then with secondary antibody for 1 h at room temperature followed by DAPI staining to detect cell nuclei (Kataria et al., 2018; Dyck et al., 2019; Hart et al., 2020). The percentage of BrdU+/DAPI+ proliferative cells among the total DAPI+ cells was quantified in 8–10 fields with an average of 300 cells per experimental condition under 20× objective.

To evaluate differentiation pattern of drNPC-O2, cells were maintained for 14 d in differentiation media. Then, cells were immunostained for β- βTIII, and GFAP to assess the proportion of neurons and astrocytes, respectively. For quantification, images of 8–10 fields were taken under 20× objective and the percentage of β-tubulin-III+/DAPI+ or GFAP+/DAPI+cells were calculated among the total number of DAPI+ cells in analyzed fields in each condition.

Assessment of neuronal maturity, complexity, and synapse formation of drNPC-derived neurons in vitro

To assess the maturity and synapse formation by drNPC-derived neurons under various conditions, drNPC-O2 were differentiated for four weeks as mentioned above on laminin or laminin+CSPGs (2.5 µg/ml). For neuronal maturity, cells were immunostained with MAP-2 (dendritic marker), GluA1 (AMPA receptor), and postsynaptic density protein-95 (PSD-95) antibodies. The density of postsynaptic scaffolding proteins and AMPA receptors on dendrites was measured using ImageJ software (Llamosas et al., 2020). Sholl analysis was performed on dendrites to assess neuronal complexity. In brief, images were taken from randomly selected neurons in each condition using a Zeiss confocal microscope. Concentric circles (soma considered as the center) were drawn with 25-µm interval. Number of dendrites intersections was used to create the Sholl plot and number of branches were plotted by ImageJ software, Simple Neurite Tracer plugin (Llamosas et al., 2020; Zhou et al., 2020). For synapse formation, neurons were immunostained with synaptophysin and PSD-95 to detect pre and postsynaptic scaffolding proteins, respectively. For each condition, 8–10 fields were randomly imaged under 20× objective using Confocal Zeiss microscope. Synaptic density was measured using ImageJ software and SynapCountJ plugin (Kucukdereli et al., 2011).

Whole-cell patch-clamp recording of drNPC-O2-derived neurons *in vitro*

For electrophysiological recording, human drNPC-O2 were differentiated for four weeks on coverslips coated with laminin or laminin+CSPGs treated with or without ILP/ISP. For whole-cell recordings, neurons were maintained in a bath solution containing 140 mM NaCl, 5 mM KCl, 2 mM $CaCl_2$, 2 mM Mg Cl_2, 10 mM HEPES-NaOH, and 10 mM glucose, pH 7.4. Micropipettes were pulled from borosilicate glass capillary tubes using a horizontal puller (Sutter Instrument P-97 micropipette puller). Before recording, micropipettes were filled with the intracellular solution containing 123 mM K-gluconate, 10 mM KCl, 1 mM $MgCl_2$, 10 mM HEPES-KOH, 1 mM EGTA, 0.1 mM $CaCl_2$, 1 mM K2-ATP, 0.2 mM Na4-GTP, and 4 mM glucose, pH 7.4. The osmolarity of intracellular solution was adjusted to 295–298 mOsm, and resistance of the filled pipettes was between 3 and 4 mΩ. Whole-cell patch-clamp recordings were collected in voltage clamp configuration using a Multiclamp 700B amplifier (Molecular Devices) and Signal software (Cambridge Electronic Design). Recordings were low pass filtered at 3 kHz and acquired at 25 kHz with CED Power 1401 AD board. Once a successful seal of the neuron was achieved, spontaneous activities were recorded for 2–3 min, while the neuron was held at –60 mv. If a stable seal or holding potential could not be obtained for 2 min, the neuron was discarded. The recordings were imported into MiniAnalysis software and EPSCs were detected within a stable time frame of 60-s in the middle of recording. In this study, we only focused on analysis of the inward current, indicating EPSC events, across treatment conditions. To specify the EPSCs signal, we blocked IPSCs using picrotoxin (a GABA blocker, 50 μM) and strychnine (a glycinergic blocker, 2 μM) as well as action potentials using tetrodotoxin (TTX; 1 μM). We further confirmed the specificity of EPSCs using AMPA receptor antagonist (CNQX).

Rat model of compressive SCI

We used a clinically-relevant model of clip-compression SCI that has been extensively characterized and employed by our group and others (Karimi-Abdolrezaee et al., 2006, 2010, 2012; Gauthier et al., 2013; Alizadeh et al., 2018; Dyck et al., 2019; Hart et al., 2020). In brief, female SD rats were deeply anesthetized by inhalation of a mixture of O_2 (2%) and isoflurane (4%) via a mask integrated into a surgical stereotaxic frame. After deep anesthesia was achieved, for maintenance, isoflurane was reduced to 2%. The surgical area was shaved and disinfected (70% ethanol and povidone iodine). Spinal column was exposed by a midline incision at the thoracic area (T5–T9), and skin and superficial tissue were retracted. The rats received laminectomy at T6–T8, and spinal cord was compressed at T7 using a 35-g aneurysm clip (University Health Network, Toronto, Ontario, Canada) for 1 min. The surgical wounds were sutured. For postsurgical pain management, animals received one dose of meloxicam (Metacam, 2 mg/kg, Boehringer Ingelheim GmbH) before their surgery followed by four injections of buprenorphine (Vetergesic, 0.03 mg/kg, Champion Alstoe Animal Health) with 8-h interval. To prevent dehydration, rats received 5 ml of sterile normal saline subcutaneously. Moreover, animals received oral Clavamox (amoxicillin plus clavulanic acid, Pfizer) for 5 d, starting 2 d before surgery to minimize the risk of urinary tract infection and surgery-induced hematuria. SCI rats were monitored daily, and their bladders were expressed manually three times a day until the regain of bladder function.

Transplantation of human caudalized drNPC-O2 and ILP/ISP treatment in rat SCI

For transplantation studies, at 14 d after SCI, animals were block randomized into four experimental groups according to their functional performance in Basso, Beattie, Bresnahan (BBB) locomotion assessment to allocate animals with equivalent deficits across all experimental groups before starting the treatments. Experimental groups included: (1) SCI/vehicle control; (2) SCI/drNPC-O2; (3) SCI/ILP+ISP; and (4) SCI/drNPC-O2/ILP+ISP (N = 10–14 rats for each group; Fig. 1*B*).

Intraspinal transplantation of drNPC-O2 was conducted based on a well-established method developed by our group (Karimi-Abdolrezaee et al., 2006, 2010; Eftekharpour et al., 2007). SCI animals were deeply anesthetized as described above. Under sterile conditions, the injured spinal cord was carefully exposed and stabilized using vertebral stabilizers to limit animal movements because of respiration during cell injections. Then 2.5×10^5 drNPC-O2 in 5-µl diluent (NWL) was stereotactically injected into the injured spinal cord tissue using a Hamilton syringe connected to a microglass pipette. Each rat received four bilateral intraspinal injections at 2 mm rostral and 2 mm caudal away from the lesion center. Assessment of cell viability by Trypan Blue staining was performed to ensure ~90% cell viability. Animals in all other experimental groups received the same number of injections to the spinal cord using only medium. At the time of drNPC-O2 transplantation, vehicle (saline) or ILP/ISP (20 µg/d) treatment was systemically delivered subcutaneously for six weeks by implantation of Alzet miniosmotic pump (catalog #2006, Alzet; Fig. 1). ILP and ISP peptides were dissolved in saline for *in vivo* delivery. To prevent immune rejection of transplanted human drNPC-O2 by the host immune system, rats received daily injection of 3 mg/kg tacrolimus (catalog #B2143, APExBio) subcutaneously until the experimental endpoint at 16 weeks post-SCI. All nontransplanted rats also received tacrolimus in the same manner as transplanted rats.

Anterograde tracing of the corticospinal tract (CST) axons

To anterogradely label the CST axons in the spinal cord, SCI animals received bilateral intracortical injections of AAV8-mCherry (catalog #7106, Vector Biolabs) two weeks before their experimental endpoint. Each rat received eight injections into the cortex per hemisphere (5×10^{12} particles/ml and 0.5 µl/injection site) over 45–60 min (Kumamaru et al., 2018). To label the majority of CST neurons in Layer V of the rat sensorimotor cortex, we used the following coordinates (in reference to bregma; Karimi-Abdolrezaee et al., 2010): (1) 1 mm anterior, 1 mm lateral; (2) 0.5 mm anterior, 1 mm lateral; (3) 1 mm posterior, 1 mm lateral; (4) 2.5 mm posterior, 1 mm lateral; (5) 0.5 mm posterior, 2 mm lateral; (6) 1.5 mm posterior, 2 mm lateral; (7) 1 mm anterior, 2.5 mm lateral; and (8) 1.5 mm anterior, 2.5 mm lateral. The depth for all injections was 1.2 mm from cortical surface.

Tissue processing and immunohistochemistry on spinal cord tissue sections

Tissue collection was performed at the study endpoint, 16 weeks post-SCI. Briefly, rats were deeply anesthetized with isoflurane/propylene glycol (60:40%; Fisher Scientific) and then transcardially perfused with cold 0.1 M PBS to remove blood. For histologic analysis, rats were then perfused transcardially with 2.5% PFA in 0.1 PBS (pH 7.4). Then, the spinal cords were excised and postfixed in 2.5% PFA and 10% sucrose solution overnight at 4°C, and further cryoprotected in 20% sucrose solution in PBS for 24–48 h at 4°C. A 2.5 cm length of the spinal cord centered at the injury site was embedded in tissue-embedding medium (Tissue-TeK CRYO-O.C.T Compound, Electron Microscopy Sciences) on dry ice and cross sections (35 µm) were serially cut on a cryostat (Leica) and stored at −80°C for further analysis (Dyck et al., 2018).

For immunohistochemistry, spinal cord sections were air-dried at room temperature for 30 min followed by rehydration with PBS for 5 min. Then, slides were permeabilized and blocked using 5% skim milk, 0.05% Triton X-100 in 0.1 PBS for 1 h at room temperature. Tissue sections were incubated overnight at 4°C with primary antibodies (Table 1) diluted in the blocking solution. All antibodies used in our immunohistochemical studies were validated for their specificity. Spinal cord sections were washed three times in PBS and incubated with appropriate secondary antibodies (Table 1) for 1 h at room temperature. For double or triple co-immunostaining, the tissue sections were incubated with a second or third primary antibody sequentially as described above. Finally, the slides were washed with PBS and stained with DAPI (1:10,000) to label nuclei (Dyck et al., 2018).

In vivo cellular assessments and quantifications

In all histologic procedures, quantification was executed in an unbiased manner by examiners blinded to the treatment groups. For evaluating the transplant volume and biodistribution, 20 cross sections with 100-µm interval were selected from each animal ($N = 4$/group) and immunostained with STEM121, a specific antibody against human cytoplasm (catalog #Y40410, Takara Bio), and imaged under 20× objective (Zeiss AxioImager fluorescent microscope). Transplant volume was assessed using unbiased Cavaliere probe (StereoInvestigator, MBF Bioscience). 3D reconstruction of transplanted cells (stained with STEM121 antibody) in the injured spinal cord was performed using Reconstruct Software (Harris et al., 2015). We also quantified the number of surviving transplanted human drNPC-O2 immunostained with HNA, a human nucleus-specific antibody (catalog #1281, Millipore), using Optical Fractionator probe (StereoInvestigator, MBF Bioscience). To assess fate specification of transplanted drNPC-O2, spinal cord cross sections were immunostained for various neural markers ($N = 5$ animal/group). For each marker, five sections were randomly selected (200- to 300-µm interval) and double-immunostained with human-specific marker (HNA or Ku80) and neural markers. From each section, 10 fields were randomly imaged under 20× objective. The percentage of positive cells for each marker was calculated among the total number of human cells (HNA+/DAPI+ or Ku80+/DAPI+ cells).

In vivo evaluation of synaptic density of engrafted drNPC-O2 in the injured spinal cord was conducted on five sections (each side) stained with synaptophysin, STEM121 and vGlut1 (for excitatory synapses) or GABAr (for inhibitory synapses). Co-localization of STEM121, synaptophysin and vGlut1 (for excitatory synapses) or GABAr (for inhibitory synapses) was quantified using Simple Neurite Tracer and SynapCountJ plugin of ImageJ software (Ippolito and Eroglu, 2010).

Assessment of *in vivo* neuronal morphology and complexity analysis

To analyze the morphologic complexity of human drNPC-O2-derived neurons, which were co-immunostained with STEM121 and NeuN, z-stake images were taken from each neuron and then reconstructed in neuTube software. Reconstructed neuronal morphology was analyzed using NeuroM package (available at www.github.com) in Jupiter Notebook platform (Markram et al., 2015; Iavarone et al., 2019).

RNA-seq for human transplanted cells

For RNA-seq of transplanted human cells in the spinal cord, at 14 weeks after transplantation, rats were euthanized under deep anesthesia with isoflurane/propylene glycol (60:40%) and were transcardially perfused with 0.1 M PBS to remove blood cells ($N = 4$ per group). One cm of spinal cord tissue (centered at the injury site) was dissected and the RNA was extracted and purified using GeneJET RNA purification kit according to the manufacture instruction (catalog #K0731, Thermo Fisher Scientific). Library preparation and RNA-seq were performed by StemCore laboratories at the Ottawa Hospital Research Institute (Ottawa, Ontario, Canada). The quality of RNA was assessed, and mRNA libraries were prepared using TureSeq RNA samples prep kit protocol and sequenced by Genome Analyzer llx (Illumina). Rat and human transcripts were separated and mapped to the corresponding genomic DNA sequences using STAR software (Söllner et al., 2017) in Galaxy workflow (Blankenberg and Hillman-Jackson, 2014; Fan et al., 2015; Grüning et al., 2017) and iDEP workflow (Ge et al., 2018). The mapped sequences were normalized by trimmed means of M value and differentially expressed genes were identified using DEseq software (adj $p < 0.05$, fold change > 2). For GO and KEGG pathway analyses p-value was set using Fisher's exact test and adjusted p-value was calculated using the Benjamini–Yekutieli method and the cutoff was 0.05.

Modulation and assessment of Wnt/β-catenin signaling

To functionally assess the effects of Wnt/β-catenin pathway activity on neuronal differentiation, drNPC-O2 (15,000 cell/cm^2) were plated on laminin and laminin+CSPGs (2.5 and 5 µg/ml) and differentiated for one week with refreshing half of the media twice a week. To verify the role of Wnt/β-catenin signaling in neuronal differentiation (i.e., loss of function), drNPC-O2 were treated with the Wnt/β-catenin inhibitor

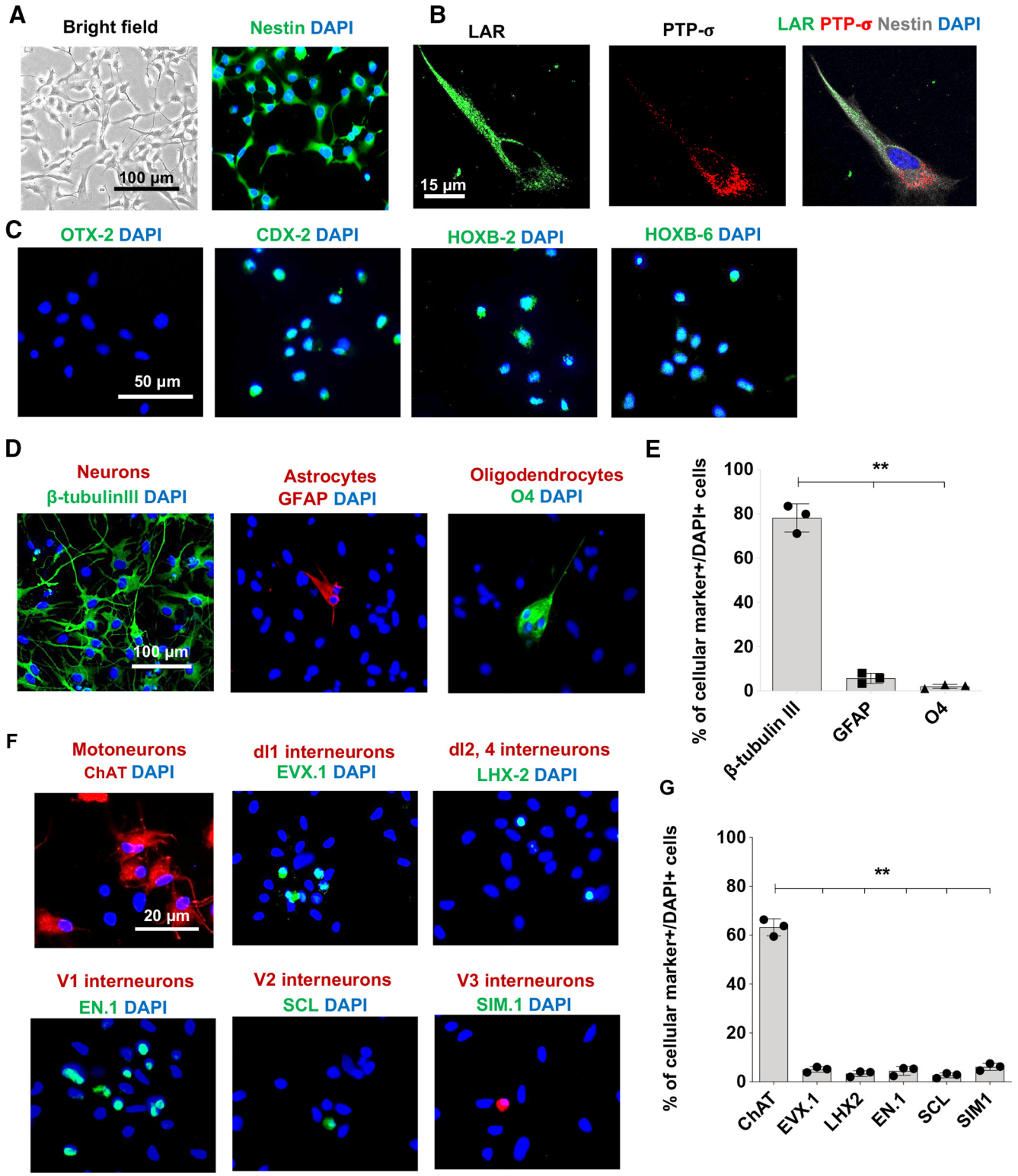

Figure 2. Human drNPC-O2 are multipotent and show caudal regional specification *in vitro*. ***A***, Immunostaining verified human drNPC-O2 express nestin, a cardinal marker of neural stem/progenitor cells. ***B***, Representative immunostaining images confirmed human drNPC-O2 express LAR and PTPσ receptors. ***C***, Immunostaining for rostral and caudal NPC markers verified that drNPC-O2 did not express the rostral NPC marker OTX2, while they expressed CDX2 (master regulator of HOX genes), HOXB2 (cervical NPCs), and HOXB6 (cervical/thoracic NPCs). ***D–E***, Upon differentiation *in vitro*, human drNPC-O2 predominantly gave rise to neurons with lower capacity for astrogenesis and oligodendrogenesis. ***F***, Immunostaining exhibited that drNPC-O2 generated spinal cord neuronal subtypes including motoneurons, dorsal interneurons, and ventral interneurons. ***G***, Quantitative analysis showed drNPC-O2 predominantly differentiated into motoneurons and also produced dI1, dI2, dI4, V1, V2, and V3 spinal interneurons. Values represent mean ± SEM, $^{**}p < 0.01$; one-way ANOVA. $N = 3$ independent experiments, 2–3 technical replicates.

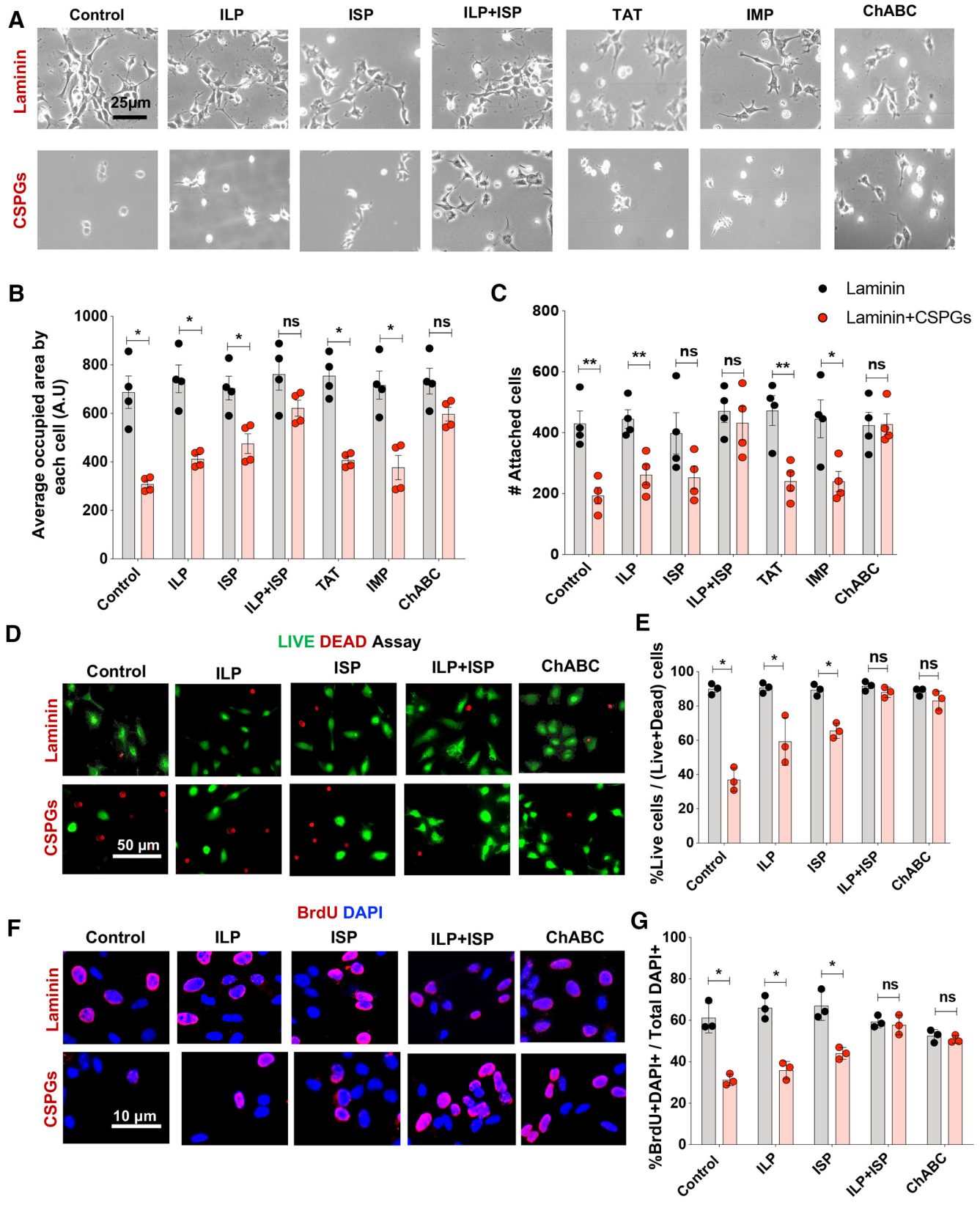

Figure 3. CSPGs inhibit properties of human drNPC-02 *in vitro* that can be reversed by co-inhibition of LAR and PTPσ receptors. ***A–C***, Spreading and attachment of human drNPC-02 were evaluated on laminin and laminin+CSPGs under various conditions by measuring total surface area and the number of attached DAPI cells at 2 d after plating. ***A***, Representative images show that CSPGs limited cell spreading and attachment of drNPC-02. ***B***, ***C***, Co-blockade of LAR and PTPσ receptors by ILP+ISP significantly reversed CSPG inhibitory effects, while ILP or ISP treatment individually had no significant effect. Specificity of ILP and ISP was confirmed as control peptides IMP and TAT had no effects on CSPGs inhibitory effects. Degradation of CSPGs by ChABC also significantly reversed CSPGs effects. ***D***, ***E***, Survival of drNPC-02 on CSPGs substrate was compared with laminin control condition using LIVE/DEAD assay at 2 d after plating. ***D***, Live cells were labeled as green (Calcein) and dead cells were labeled as red (EthD-1). ***E***, CSPGs significantly decreased drNPC-02 survival compared with the laminin control condition. Although ILP or ISP solitary treatment slightly increased drNPC-02 survival, only ILP+ISP co-treatment could significantly reverse CSPGs inhibitory effects on cell survival. ChABC also significantly restored

IWR1 (5 μM; catalog #I0161 Sigma-Aldrich). IWR1 compound directly interacts with the destruction complex protein Axin2 and stabilizes it, which results in destruction of β-catenin complex (Liu et al., 2017; Martins-Neves et al., 2018). To activate Wnt/β-catenin signaling, drNPCs were treated with a Wnt/β-catenin activator CHIR99021 (2 μM; catalog #SML1046, Sigma-Aldrich), small molecule. CHIR99021 small molecule specifically and efficiently inhibits glycogen synthase kinase-3 (GSK-3), which is a negative regulator of Wnt/β-catenin signaling pathway (Mulligan and Cheyette, 2012; Wu et al., 2015). After one week, differentiated drNPC-O2 were fixed and immunostained with GFAP and β-tubulin-III to assess fate specification. To evaluate the activity of Wnt/β-catenin pathway, differentiated drNPC-O2 were immunostained with β-catenin antibody and nuclear localization of β-catenin components (as an indicator for Wnt/β-catenin activity) was quantified using ImageJ software (Zhang et al., 2011; Hendaoui et al., 2014; Cui et al., 2019).

Neurobehavioral assessments

All neurobehavioral evaluations were performed and analyzed by two examiners who were blinded to the animals' treatments.

BBB open field locomotor score

Open field BBB locomotor rating scale was used to evaluate longitudinal hindlimb motor function weekly from week 1 to week 15 post-SCI (Basso et al., 1995). Briefly, SCI rats were placed individually on a flat nonslippery surface and permitted a few minutes to acclimatize to their surroundings. Rats were observed for 4–5 min individually and given a score denoting the degree of motor function. BBB is a 22-point (0–21) scale that assesses hindlimb locomotor recovery including joint movements, stepping ability, coordination, as well as trunk stability. BBB scoring was performed by two examiners who were blinded to the animals' treatments.

Grid-walking analysis

Sensorimotor integrity of animals was evaluated by performing grid-walk analysis on weeks 11, 13, and 15, when most injured rats began to show adequate weight support. For this analysis, animals crossed a 10-cm-wide and 1-m-long horizontal grid runway which was elevated 30 cm from the ground. For grid-walking assessment, each animal was trained before the injury. Animals were tested in three trials and recorded on a digital videotape. To quantify this analysis, the average number of foot errors was counted within an identified 70-cm length of the grid runway and in each session, the average number of complete hind-paw falls of each rat was taken from the three trials. In uninjured animals (baseline), no foot errors were detected. The animals without weight support showed the maximum number of foot falls (11) in this assessment as we described previously (Karimi-Abdolrezaee et al., 2006, 2010).

Assessment of pain response after SCI

To assess pain sensitivity to mechanical and thermal stimuli, von Frey and tail flick tests were performed on weeks 11, 13, and 15 post-SCI. Briefly, for mechanical pain response von Frey filament was pressed perpendicularly to the dorsal paw in between the first and second metatarsals ~1 cm proximal to the joint. The monofilament was applied in a smooth and steady manner for 3 s then removed with 30-s interval between every two filaments. A positive response occurs when the rat quickly moves the paw away from the stimulus. All rats were first tested using a 4.56 filament. For a negative response, the next larger filament was used, and when a positive response was elicited, the next smaller filament was tested to validate the response. The threshold of avoidance response (jumping, escaping, vocalization and reacting in an aversive manner) was recorded. Once a particular filament elicited two consecutive positive responses, or two out of three trials gave a positive response, that filament was recorded as the animal's pain threshold. Both hind paws were tested individually and the average pain threshold of the two paws was used to represent one individual animal pain score. Thermal pain response was examined by tail flick in response to immersion of 5 cm of the end of the tail in a 46°C water bath. The latency of the rat to remove its tail from the heat was recorded. Three attempts were made per animal in each session and each attempt was separated by a 20-s interval period. The latency period of response after stimulus was recorded and compared across all groups.

Statistical analysis

All analyses were performed unbiasedly by randomization and blinding. Prism 6 software was used for statistical analysis. To compare data between two groups nonparametric Student's *t* test (columnar analysis) and multiple *t* test (grouped analysis) were used. For comparing more than two groups, nonparametric one-way ANOVA (Kruskal–Wallis test) was used. For Sholl analysis two-way ANOVA repeated measure followed by Tukey's *post hoc* test was conducted. For behavioral analyses, two-way ANOVA followed by Fisher's LSD *post hoc* was conducted. The data are reported as mean ± SEM, and $p \geq 0.05$ was considered statistically significant.

Results

CSPGs suppress the neurogenic capacity of human drNPC-O2 through activation of LAR and PTPσ receptors *in vitro*

We previously showed that CSPGs inhibits several key properties of mouse-derived adult NPCs through activation of LAR and PTPσ receptors (Dyck et al., 2015, 2019). To verify whether CSPG signaling regulates the behavior of human caudalized drNPC-O2, we conducted a series of *in vitro* experiments. We exposed drNPC-O2 to laminin (representing a permissive substrate) or laminin+CSPGs (representing SCI matrix). First, using immunocytochemical assessments, we confirmed that human drNPC-O2 express nestin, the cardinal marker of multipotent NPCs, on the laminin control substrate under growth factor media (Fig. 2*A*). Next, we verified that human drNPC-O2 express LAR and PTPσ receptors, and as such they can respond to CSPGs in their environment (Fig. 2*B*). Furthermore, we verified that drNPC-O2 express signature markers of caudalized spinal NPCs including CDX-2 (master regulator of HOX genes), HOXB-2 (cervical NPCs marker), and HOXB-6 (cervical/thoracic NPCs marker), while lacking OTX2 expression, a marker of rostral NPCs (Fig. 2*C*).

Following these verifications, we assessed the neurogenic capacity of caudalized drNPC-O2. After two weeks of differentiation on the baseline laminin substrate, drNPC-O2 predominantly generated neurons (β-tubulin-III, 78.16 ± 6.34%) with a small percentage of astrocytes (5.76 ± 2.30%) and oligodendrocytes (2.16 ± 0.89%), indicating their neuronal commitment (Fig. 2*D*,*E*). Then, we evaluated whether drNPC-O2 were able to differentiate into motoneurons and spinal cord-specific interneurons. Immunocytochemical studies confirmed drNPC-O2 can differentiate to motoneurons (ChAT+, 62.25 ± 3.49%), as well as spinal interneurons including dI1 (EVX.1+, 5.06 ± 1.12%), dI2,4 (LHX2+, 3.37 ± 1.19%), V1 (EN.1+, 2.41 ± 1.79%), V2 (SCL+, 1.66 ± 1.01%), and V3 (SIM.1+, 5.13 ± 1.44%; Fig. 2*F*,*G*).

Next, we determined the effects of CSPGs on key properties of human drNPC-O2 such as cell spreading, survival, proliferation and differentiation (Fig. 1). We exposed drNPC-O2 to an enriched CSPGs substrate that recapitulates the post-SCI milieu. The CSPGs mixture comprised of aggrecan, neurocan, versican,

←

CSPGs effects on cell proliferation. ***F***, ***G***, BrdU incorporation and quantitative immunocytochemistry showed proliferation of drNPC-O2 was significantly declined on CSPGs, and ILP+ISP co-treatment or ChABC treatment significantly reversed these effects. Values represent mean ± SEM, $^*p < 0.05$; multiple *t* test. $N = 3$–4 independent experiments, 2–3 technical replicates. ns: non-significant.

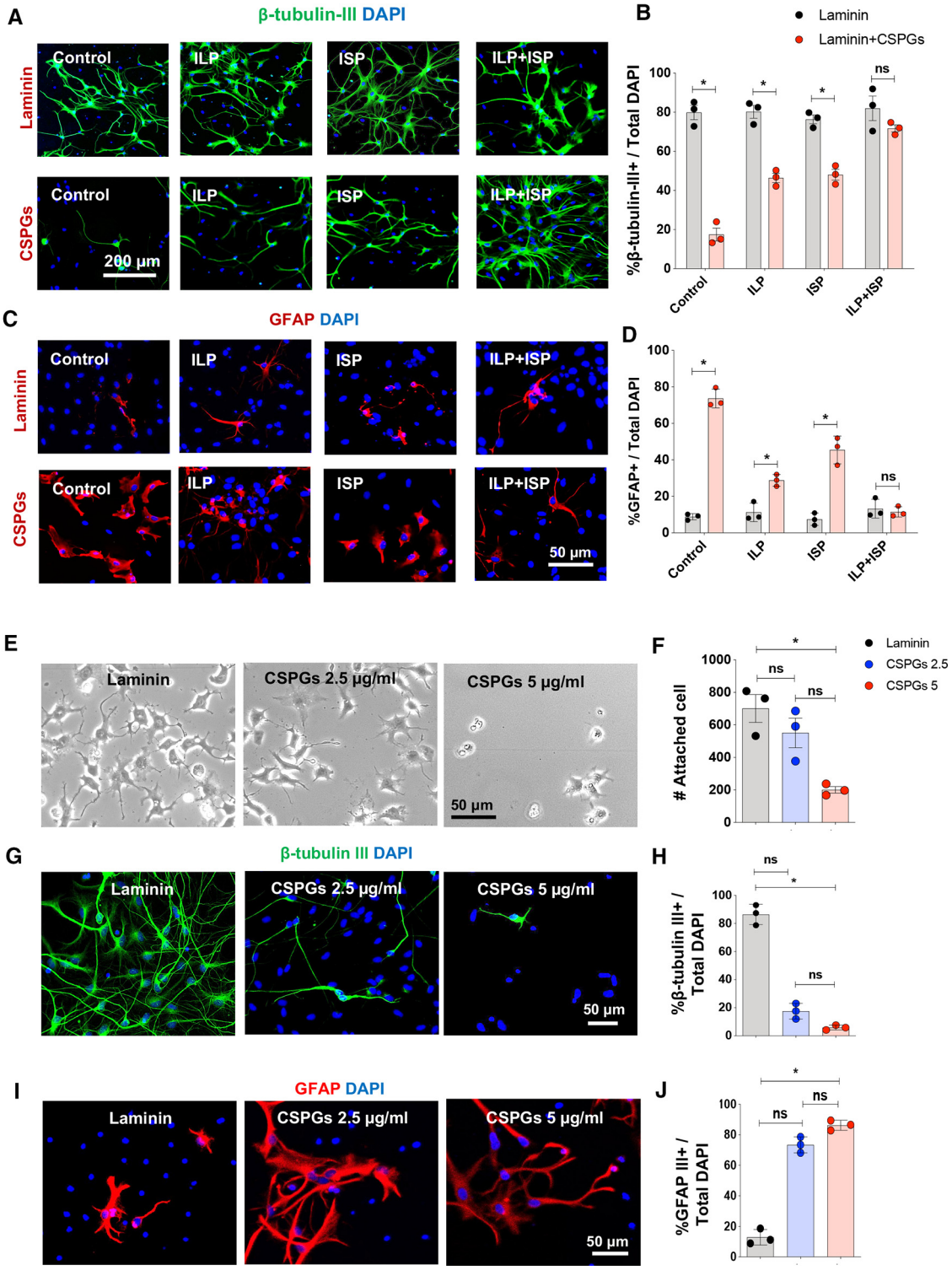

Figure 4. CSPGs impede neuronal differentiation, while increase astrocyte differentiation of human drNPC-02 through co-activation of LAR and PTPσ. ***A***, ***B***, Immunocytochemical assessment of drNPC-02 on laminin and laminin+CSPGs using β-tubulin-III and DAPI showed that CSPGs limit neuronal differentiation through LAR and PTPσ receptors. Values represent mean ± SEM, *$p < 0.05$; multiple *t* test, $N = 3$ independent experiments, 2–3 technical replicates. ***C***, ***D***, GFAP immunostaining and quantification two weeks after differentiation of drNPC-02 indicated that CSPGs promote astrogenesis compared with the control laminin condition, and ILP/ISP co-treatments can reverse these effects. Values represent mean ± SEM, *$p < 0.05$; multiple *t* test, $N = 3$ culture experiments. ***E***, ***F***, CSPGs restrict attachment and fate specification of drNPC-02 in a concentration dependent manner. ***E***, Bright-field images of drNPC-02 on laminin and laminin/CSPGs (2.5 and 5 µg/ml) after 2 d. ***F***, Although CSPGs 5 µg/ml significantly reduced the number of attached drNPC-02, CSPGs 2.5 µg/ml did not affect cell attachment. ***G–J***, Immunostaining for β-tubulin-III and GFAP show CSPGs significantly reduced neurogenesis at 5 µg/ml concentrations compared with control laminin condition while promoting astrogenesis. Values represent mean ± SEM, *$p < 0.05$; one-way ANOVA-multiple comparison, test $N = 3$ culture experiments. ns: non-significant.

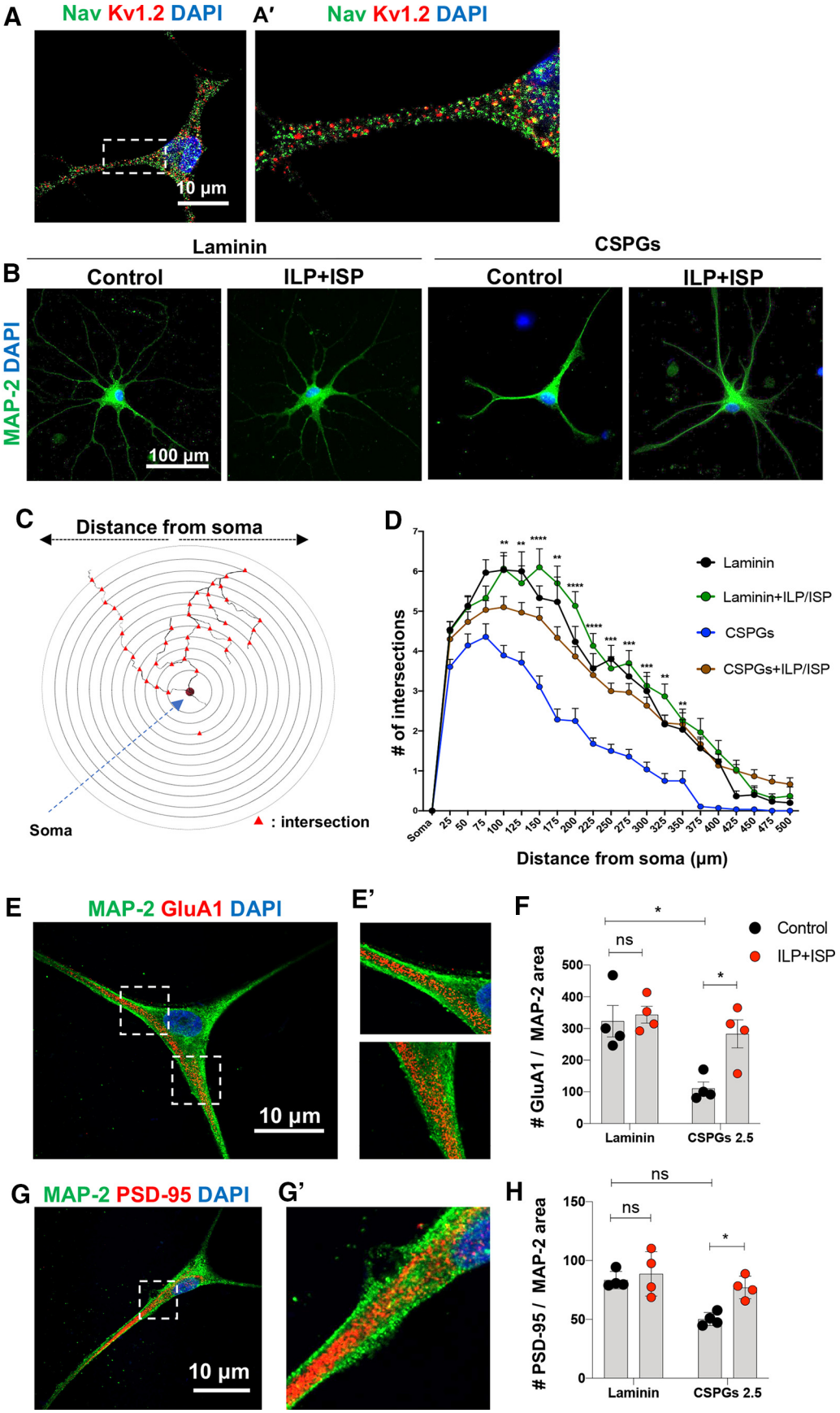

Figure 5. CSPG/LAR/PTPσ axis hinders dendritic arborization and maturity of drNPC-O2-derived neurons. ***A***, Representative immunostaining images show expression of pan-Na and Kv1.2 potassium channels in drNPC-O2-derived neurons after four weeks of differentiation. ***B***, Immunostaining of drNPC-O2-derived neurons for the dendritic marker MAP-2 verified neuronal maturity. ***C***, ***D***, Dendritic complexity of drNPC-O2-derived neurons was compared on laminin and laminin+CSPGs substrates. ***C***, Schematic figure of Sholl analysis illustrates dendritic arborization and

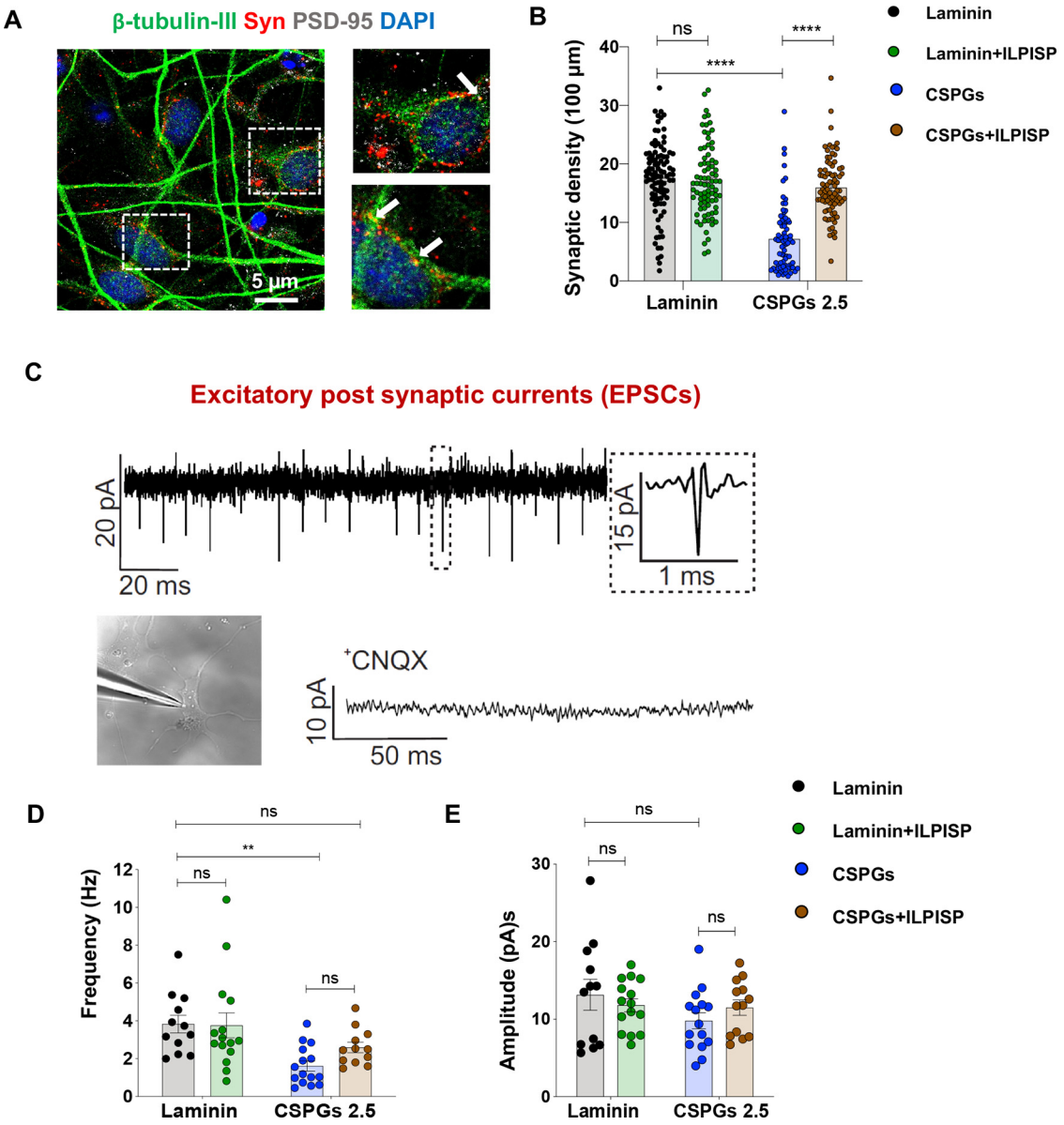

Figure 6. CSPGs decrease synapse formation and spontaneous activity of drNPC-O2-derived neurons through activation of LAR and PTPσ receptors. ***A***, ***B***, Synaptic density was assessed by co-immunostaining for β-tubulin, presynaptic (synaptophysin) and postsynaptic (PSD-95) markers. ***F***, Quantification of synaptophysin/PSD-95 co-localization indicated that CSPGs decreased synapse formation and ILP/ISP co-treatment was able to significantly reverse these effects. Values represent mean ± SEM, *$p < 0.05$; one-way ANOVA, $N = 4$, 20–25 neurons per condition (each N). ***C***, Electrophysiological recording of EPSC of drNPC-O2-derived neurons in presence of picrotoxin (50 μM) for blocking GABAergic synapses, strychnine (2 μM) for blocking glycinergic synapses and TTX (1 μM) to block action potentials. Specificity of EPSC recording was further verified by using AMPA receptor antagonist (CNQX), which completely abolished EPSC events. ***D***, CSPGs significantly decreased frequency of spontaneous neuronal activity and ILP/ISP co-treatment moderately (but not significantly) improved it. ***E***, CSPGs and/or ILP/ISP treatment did not affect amplitude of spontaneous activity in neurons. Values represent mean ± SEM, *$p < 0.05$; one-way ANOVA. $N = 3$, 5 neurons per condition. ns: non-significant.

←

branching. ***D***, Sholl analysis showed that ILP/ISP co-treatment reversed the repressing effects of CSPGs on neuronal maturity and increased the number of branches within 100–350 µm away from the soma. Values represent mean ± SEM, *$p < 0.05$; two-way ANOVA followed by Tukey's multiple comparison test, $N = 3$, 10–12 neurons per condition. ***E***, ***E′***, Neuronal maturity was assessed under various conditions by immunocytochemical analysis of GluA1 (AMPA receptor) and MAP-2 (dendritic marker). ***F***, Quantitative analysis revealed that CSPGs reduced density of GluA1 receptor on dendritic branches and blocking LAR and PTPσ receptors reversed CSPGs inhibitory effects. ***G***, ***G′***, Confocal imaging of PSD-95 (postsynaptic marker) and MAP-2 co-immunostaining for neuronal maturity analysis. ***H***, Analysis of PSD-95 density on dendrites also showed that CSPGs declined (not significantly) PSD-95 density on dendritic area and co-blockade of LAR and PTPσ receptors using ILP/ISP resorted these CSPGs suppressing effects. Values represent mean ± SEM, *$p < 0.05$; multiple t test. $N = 4$ independent experiments. ns: non-significant.

and phosphocan that represent key CSPG variants in the ECM of SCI. We included laminin in the CSPGs substrate as it is also a component of injury matrix (Cregg et al., 2014; Alizadeh et al., 2019). Using this SCI relevant matrix, we assessed the effects of CSPGs on human drNPC-O2. To identify whether LAR and PTPσ receptors mediate the effects of CSPGs on human drNPC-O2, we targeted these receptors in NPCs with their specific intracellular inhibiting peptides, ILP and ISP, respectively. Using an unbiased stereology-based method, we first showed CSPGs significantly decrease (~55%) the ability of human drNPC-O2 to spread their processes and attach to the substrate compared with laminin control condition, which was significantly reversed only when both LAR and PTPσ receptors were blocked with ILP and ISP simultaneously (Fig. 3*A–C*). In LIVE/DEAD assay, presence

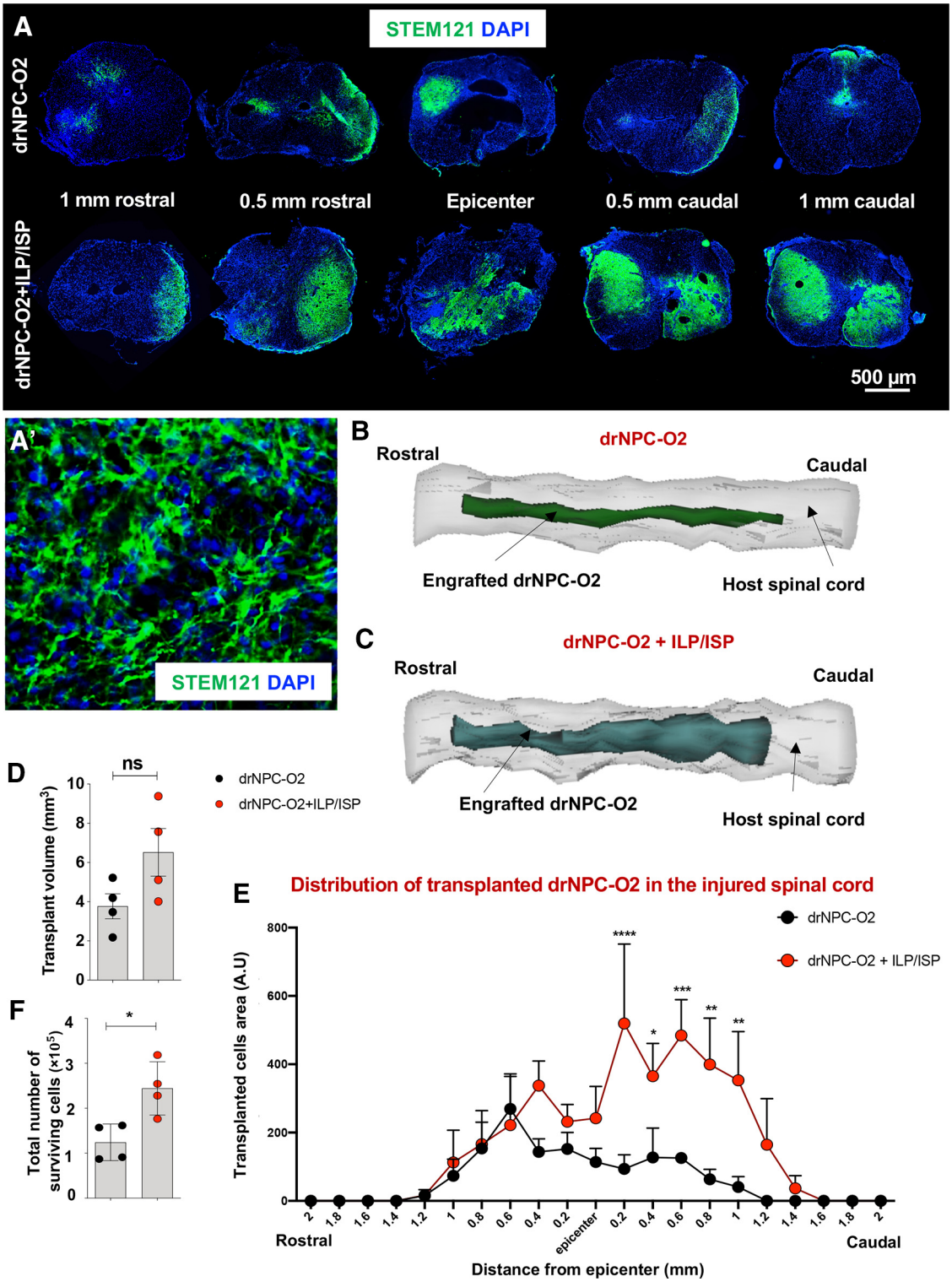

Figure 7. Co-inhibition of LAR and PTPσ receptors increases transplant volume, cell survival, and biodistribution of transplanted human drNPC-O2 in SCI. ***A–C***, ILP/ISP co-treatment improved overall transplant volume and long-term cell survival of drNPC-O2, 14 weeks after transplantation. ***A***, Immunohistochemistry for STEM121 antibody, a specific antibody for human cells, was used to detect transplanted human drNPC-O2 in the injured spinal cord of rats. ***A'***, Higher magnification of engrafted human drNPC-O2 immunostained with STEM121 show their integration and process extension in the host injured spinal cord. ***B***, ***C***, 3D reconstruction of engrafted human drNPC-O2 in the host injured spinal cord of rats is illustrated 14 weeks after transplantation. ***D***, ***E***, Quantification of transplant volume by StereoInvestigator Cavalieri probe revealed while LAR and PTPσ co-blockade by ILP/ISP treatment had no significant effects on the overall occupied area by engrafted drNPC-O2, it significantly promoted transplant volume of drNPC-O2 at 0.2-, 0.4-, 0.6-, 0.8-, and 1-mm caudal distances from the injury epicenter. ***F***, Quantitative assessment by StereoInvestigator Optical Fractionator probe showed ILP/ISP co-treatment also promoted the total number of surviving transplanted cells. Values represent mean ± SEM, $^*p < 0.05$; nonparametric Student's *t* test, $N = 4$ animals. ***F***, Analysis by StereoInvestigator Cavalieri probe showed that significantly increased. Values represent mean ± SEM, $^*p < 0.05$; two-way ANOVA followed by Fisher's LSD *post hoc* test, $N = 4$ animals. ns: non-significant.

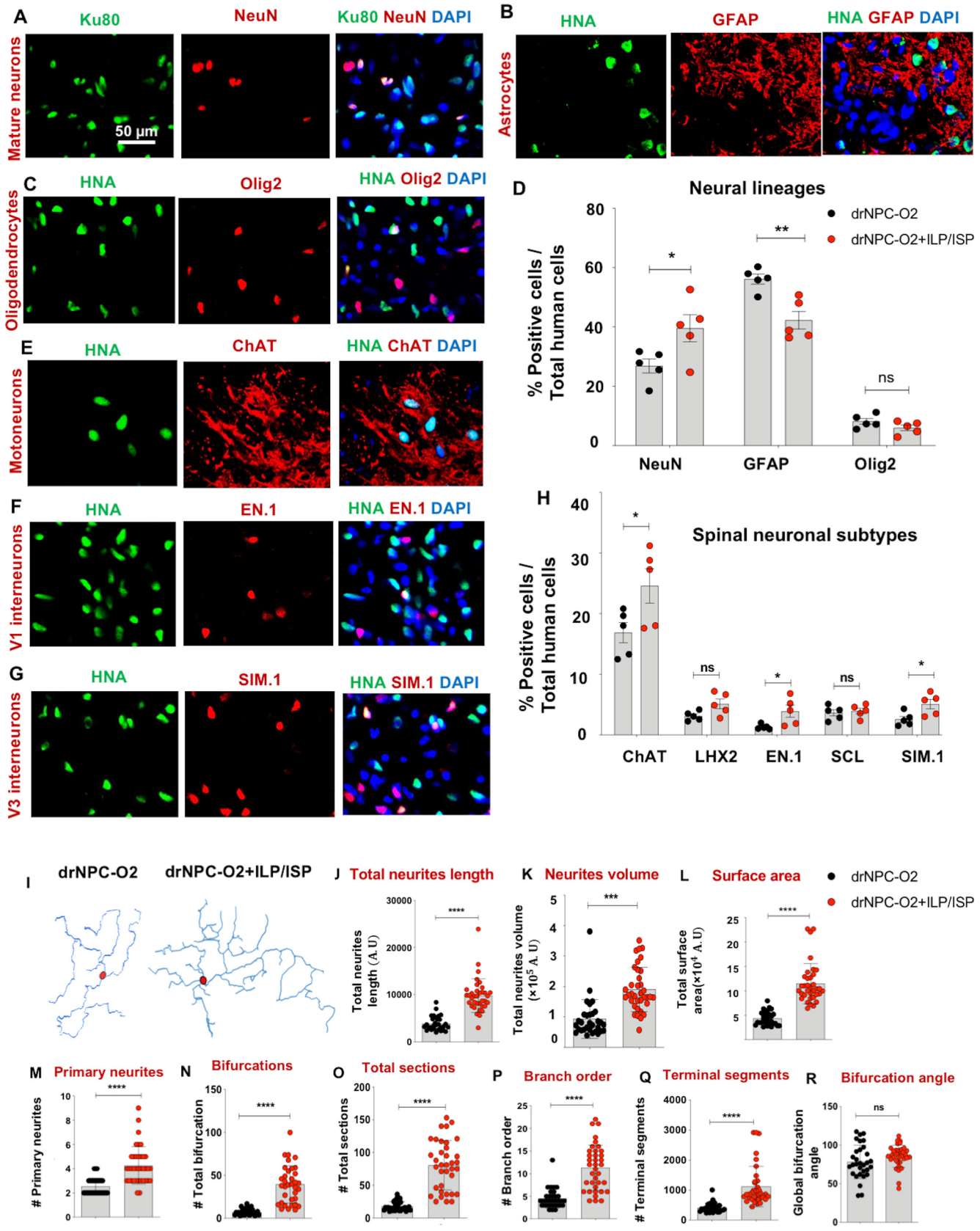

Figure 8. Co-inhibition of LAR and PTPσ enhances neuronal differentiation, morphologic complexity, and arborization of drNPC-O2-derived neurons in the injured spinal cord. ***A–D***, ILP/ISP co-administration promoted neuronal differentiation of drNPC-O2 while decreased their astrocyte differentiation. ***A–C***, Representative images of co-immunostaining of engrafted drNPC-O2 using HNA or Ku80 human nuclei antigen and NeuN (mature neuron marker), GFAP (astrocyte marker), and Olig2 (oligodendrocyte marker) are depicted. ***D***, Quantitative analysis showed ILP/ISP treatment significantly promoted neuronal differentiation of transplanted drNPC-O2 compared with vehicle treated rats. This was associated with a decrease in astrocyte differentiation under ILP/ISP co-treatment while oligodendrogenesis remained unchanged. ***E–H***, Immunohistochemical analysis indicated that ILP/ISP co-treatment significantly increased the number of ChAT-

of CSPGs also limited survival of human drNPC-O2 (52.97%) compared with laminin, which was reversed by ILP/ISP co-treatment (Fig. 3*D*,*E*). Furthermore, BrdU incorporation assay showed CSPGs significantly (22.97%) suppress drNPC proliferation, which was restored to the basal levels in laminin condition by co-treatment with ILP/ISP (Fig. 3*F*,*G*). In all these assessments, the direct inhibitory effects of CSPGs on drNPC-O2 were also significantly restored with ChABC enzyme that degrades the glycosaminoglycan side chains of CSPGs. Specificity of ILP and ISP in reversing the inhibitory effects of CSPGs on drNPC-O2 was also verified, as IMP control peptide and TAT peptide had no effect in these experiments. Collectively, these findings suggest CSPGs restrict drNPC-O2 and activation of both LAR and PTPσ is necessary to mediate the inhibitory effects of CSPGs.

Activation of CSPGs/LAR/PTPσ axis suppresses differentiation, maturation, synapse formation and spontaneous activity of drNPC-O2-derived neurons *in vitro*

We next determined whether CSPGs signaling regulates fate specification of human drNPC-O2 and particularly their differentiation into neurons. Immunocytochemical analysis showed exposure to CSPGs significantly declined neuronal differentiation of human drNPC-O2 (62.38%; Fig. 4*A*,*B*) with a concomitant increase in their astrocyte differentiation (64.82%; Fig. 4*C*, *D*). Importantly, suppressive effects of CSPGs on neuronal differentiation was mediated by both LAR and PTPσ receptors, as their co-blockade with ILP/ISP was required to reverse these effects (Fig. 4*A*,*B*). Interestingly, we identified that CSPGs influence the properties of human drNPC-O2 in a concentration dependent manner. While 5 µg/ml of CSPGs suppressed cell attachment, spreading and neuronal differentiation of human drNPC-O2, at 2.5 µg/ml concentration CSPGs only partially and not significantly inhibited neuronal differentiation of drNPC-O2 without altering their ability to attach or grow *in vitro* (Fig. 4*E*–*J*). This observation is important as in the injured spinal cord, CSPGs expression also follows a decremental gradient from the injury center toward the penumbra of the injury rostrally and caudally (Karimi-Abdolrezaee et al., 2010; Andrews et al., 2012). Thus, our *in vitro* results suggest that lower concentration of CSPGs can still affect the regenerative response of drNPC-O2 and the properties of their neuronal derivatives in distant regions from the injury epicenter.

We also examined whether CSPGs regulate the maturity of drNPC-O2-derived neurons. Our *in vitro* characterization showed these neurons express pan sodium (Nav) and potassium Kv1.2 channels after four weeks of differentiation, indicating their maturity (Fig. 5*A*,*A'*). Interestingly, Sholl analysis determined that CSPGs repress dendritic arborization and complexity of drNPC-O2-derived neurons (Fig. 5*B*–*D*). Moreover, immunocytological analyses showed CSPGs decrease the density of AMPA receptors (GluA1) and postsynaptic scaffolding protein (PSD-95) on dendrites by 65.67% and 39.78%, respectively, suggesting inhibitory effects of CSPGs on neuronal maturity (Fig. 5*E*–*H*). LAR and PTPσ were both involved in these effects as ILP/ISP co-treatment was required to significantly improve neuronal maturity and dendritic morphogenesis of human neurons exposed to CSPGs. These experiments indicate that CSPG/LAR/PTPσ axis inhibits neuronal maturation and potentially function.

Given these findings, we extended our studies to investigate whether CSPGs regulate synaptogenesis of neurons. Co-localization analysis of synaptophysin (presynaptic) and PSD-95 (postsynaptic scaffolding protein) immunolabeling in neurons revealed that persistent exposure to CSPGs causes a significant decline (59.1%) in the density of newly formed synapses, which was partially recovered by ILP/ISP co-treatment (Fig. 6*A*,*B*). Importantly, we confirmed that co-inhibition of LAR and PTPσ receptors did not interfere with baseline synaptogenesis of drNPC-O2-derived neurons on laminin control substrate. This verification was critical as LAR and PTPσ are implicated in synapse formation in neurodevelopment (Takahashi and Craig, 2013; Fig. 6*B*).

Since we found CSPGs inhibit neuronal maturation and synapse formation in neurons, we next investigated the effects of CSPGs on neuronal EPSCs which is represented as inward events in our recordings (Fig. 6*C*). Whole-cell EPSC recording demonstrated that exposure to CSPGs results in a significant reduction in the frequency (Fig. 6*D*) of neuronal spontaneous activity compared with laminin control condition, with no effect on amplitude (Fig. 6*E*). ILP/ISP co-treatment was able to partially, but not significantly, improve the frequency of neuronal activity on CSPGs (Fig. 6*D*). Collectively, these observations indicate that LAR and PTPσ receptors mediate CSPGs inhibitory effect on neuronal differentiation, arborization, morphologic complexity and maturity and synapse formation, and partially modulate the inhibitory effects of CSPGs on frequency of spontaneous activity of drNPC-O2-derived neurons.

Co-inhibition of LAR and PTPσ enhances graft survival and neuronal replacement by transplanted human drNPC-O2 in rat SCI

Replacement of functionally integrated neurons remains elusive in SCI repair. Since we found CSPGs inhibit neurogenesis and neuronal growth and maturity by co-activation of LAR and PTPσ *in vitro*, we next investigated whether co-ILP/ISP treatment could promote the potential of transplanted human drNPC-O2 in replacing spinal neurons in SCI. In a widely accepted preclinical model of compressive/contusive SCI in rats, at two weeks post-SCI, we delivered ILP/ISP systemically (20 µg/d each) in conjunction with intraspinal transplantation of human drNPC-O2 (Fig. 1). At 14 weeks after transplantation, we immunohistochemically analyzed the survival, distribution and biological properties of transplanted drNPC-O2. Our unbiased stereological analysis for STEM121+ cells (human-specific marker; Fig. 7*A*–*C*) indicated that ILP/ISP treatment partially but not significantly enhanced overall occupied transplant volume (1.73-fold; Fig. 7*D*). However, our regional analysis along the rostro-caudal axis showed co-ILP/ISP treatment significantly promoted transplant volume of drNPC-O2 at caudal distances from the SCI lesion

←

expressing motoneurons, EN.1 V1, and SIM.1 V3 spinal interneurons compared with vehicle treatment. Values represent mean ± SEM, *$p < 0.05$; multiple *t* test, $N = 5$ rats/group. ***I***, Representative reconstructed images generated from z-stack confocal imaging of drNPC-O2-derived neurons (co-immunostained with STEM121/NeuN) is depicted using Blender software. ***J–R***, Quantification of macromorphological values extracted from NeuroM morphology analysis software showed that ILP/ISP treatment significantly enhanced total neurite length, neurite volume, occupied surface area by neurons, number of primary neurites, number of bifurcations, secondary and tertiary sections and branch order indicating that co-inhibition of LAR and PTPσ improved neuronal complexity and arborization. ***Q–R***, Inhibiting LAR and PTPσ receptors also significantly increased number of terminal distal segments in neurons as another evidence for advanced geomorphological parameter of neurons. ***R***, ILP/ISP treatment did not affect global bifurcation angel of neurons. Values represent mean ± SEM, *$p < 0.05$; nonparametric Student's *t* test, $N = 8$–10 neurons per animal and 3 animals per group. ns: non-significant.

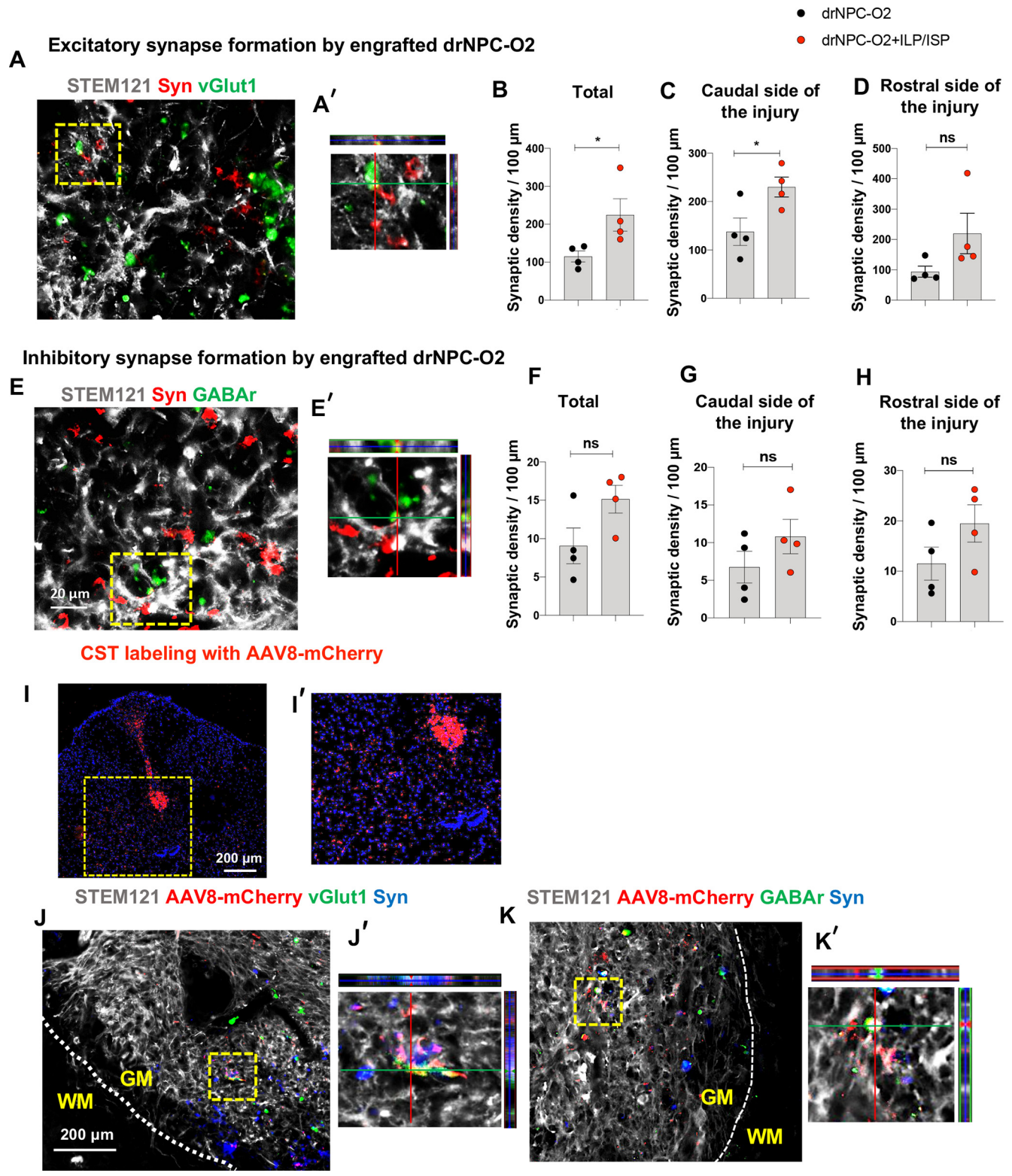

Figure 9. Neurons derived from transplanted drNPC-O2 form excitatory and inhibitory synapses within the spinal cord and with the descending corticospinal tract axons. ***A***, ***A′***, Immunohistochemical analysis of engrafted drNPC-O2 identified by STEM121 showed expression of synaptophysin (presynaptic marker) and vGlut1 (marker for excitatory synapses) in drNPC-O2-derived neurons in the ventral gray matter of spinal cord indicating that they were connected to each other through excitatory synapses. ***B–D***, Evaluation of excitatory synapse formation by transplanted drNPC-O2 was measured by quantification of STEM121, vGlut1 and synaptophysin co-localization. ***B***, Co-blockade of LAR and PTPσ receptors significantly increased total excitatory synaptic density formed by transplanted drNPC-O2 in SCI (***C***) particularly in caudal side of the injury. ***D***, Although ILP/ISP co-treatment increase excitatory synaptic density at rostral side of the injury, the difference was not statistically significant. ***E***, ***E′***, Immunostaining showed that drNPC-O2-derived neurons also formed inhibitory synapses in the ventral gray matter of spinal cord as they showed co-localization of synaptophysin and GABAr. ***F–H***, Assessment of inhibitory synapses by transplanted human drNPC-O2 was performed by quantification of STEM121, GABAr, and synaptophysin co-localization. Comparing density of inhibitory synapses formed by engrafted drNPC-O2 indicated that ILP/ISP co-treatment moderately (but not significantly) increased (***F***) total, (***G***) caudal, and (***H***) rostral inhibitory synaptic density of drNPC-O2 after transplantation. ***I***, ***I′***, Representative image of the spinal cord shows CST labeling by AAV8-mCherry at 1.2 cm rostral to the lesion site. ***J–K′***, Images show CST axons labeled with AAV8-mCherry innervate the engrafted area in the spinal cord ventral gray matter and form excitatory

injury center (5.55-fold at 0.2 mm, 2.89-fold at 0.4 mm, 3.85-fold at 0.6 mm, 6.31-fold at 0.8 mm, and 8.66-fold at 1 mm; Fig. 7*E*). Importantly, ILP/ISP adjunct treatment significantly increased cell survival of transplanted drNPC-O2 (1.96-fold) compared with the control group that only received drNPC-O2 transplantation (Fig. 7*F*). Collectively, these findings show that inhibition of CSPGs signaling can enhance long-term survival and biodistribution of human drNPC-O2 in transplantation strategies.

We next evaluated the differentiation pattern of transplanted human drNPC-O2 in the injured spinal cord. Immunohistochemical analysis of engrafted human cells revealed that drNPC-O2 gave rise to all three neural lineages. Under vehicle condition, drNPC-O2 differentiated into 26.86 ± 5.27% neurons, 57.94 ± 5.65% astrocytes and 8.17 ± 2.21% oligodendrocytes in which astrocyte differentiation predominates (Fig. 8*A–D*). Interestingly, co-inhibition of LAR and PTPσ receptors was able to significantly promote neuronal differentiation of drNPC-O2 by 12.71% compared with vehicle treated transplanted rats (Fig. 8*A–D*). Concurrently, ILP/ISP co-treatment resulted in a significant decline in astrocyte differentiation (13.88%) of transplanted drNPC-O2, while oligodendrocyte differentiation remained unaffected (Fig. 8*A–D*). Further characterization of drNPC-O2-derived neurons showed their maturation into motoneurons and spinal cord-specific V1, V2, and V3 interneurons in the injured spinal cord. Comparative analyses indicated that co-ILP/ISP treatment significantly enhanced neuronal differentiation of drNPC-O2 into ChAT-expressing motoneurons (1.45-fold), EN.1+ V1 spinal interneurons (2.94-fold), SIM.1+ V3 spinal interneurons (1.97-fold) in relation to control transplanted group, while did not affect dl2/dl4 (LHX-2+) and V2 interneurons (SCL+) populations (Fig. 8*E–H*). Taken together, our findings demonstrate that human drNPC-O2 have the potential to generate spinal cord-specific neurons and co-inhibition of LAR and PTPσ receptors can augment long-term survival, integration, biodistribution and neuronal differentiation of human drNPC-O2, in particular motoneurons and V1 and V3 spinal interneurons after SCI.

Co-blockage of LAR and PTPσ receptors promotes maturity and morphologic complexity of human drNPC-O2-derived neurons in the injured spinal cord

Maturation and process outgrowth of newly formed neurons are important for their functional integration within the neural circuit. Thus, we conducted an in-depth morphologic analysis of human drNPC-O2-derived neurons in the injured spinal cord under control and co-ILP/ISP treatment. Using z-stack confocal images, we analyzed morphologic features of human derived STEM121+/NeuN+ neurons, which were extracted through NeuroM software (Markram et al., 2015; Fig. 8*I*). Single cell morphologic analysis of new neurons revealed that co-ILP/ISP treatment significantly increased total neurite length (2.52-fold), total neurites volume (2.03-fold), total occupied surface area (2.65-fold), primary neurites (1.68-fold), bifurcations (5.58-fold), sections (4.47-fold), and number of branch order (2.63-fold) by each neuron compared with vehicle treated transplanted groups (Fig. 8*J–P*), suggesting co-inhibition of LAR and PTPσ receptors can promote neuronal arborization and expansion of 3D neuronal structure after SCI. Likewise, ILP/ISP co-treatment significantly increased number of distal segments (terminal segments) of neurons as an index of neuronal complexity by 2.73-fold, while had no effects on global bifurcation angel of these neurons (Fig. 8*Q*,*R*). Collectively, our comprehensive *in vivo* morphologic analyses of drNPC-O2-derived neurons suggest that CSPGs signaling through LAR and PTPσ receptors can negatively affect neuronal maturity and arborization after cellular transplantation, and modulation of these receptors may facilitate neuronal integration and connectivity following SCI.

Transplanted human drNPC-O2-derived neurons form inhibitory and excitatory synapses and integrate with the host descending corticospinal tract axons after SCI

We next asked whether motoneurons and spinal interneurons derived from transplanted human drNPC-O2 were able to integrate into the host neural network by forming inhibitory and excitatory synapses and connecting with descending CST axons, and whether ILP/ISP co-treatment had any effects on their synaptogenesis potential. To examine synapse formation, we performed triple-immunolabeling for human STEM121, the presynaptic marker synaptophysin and vGlut1 (for excitatory synapses; Fig. 9*A*,*A'*) or GABA(A) α1 receptor (GABAr, for inhibitory synapses; Fig. 9*E*,*E'*). We found co-localization of synaptophysin and vGlut1 as well as synaptophysin and GABAr in human drNPC-O2-derived neurons indicating they form both excitatory and inhibitory synapses. Interestingly, co-blocking LAR and PTPσ receptors significantly increased the total density of excitatory synapses (1.95-fold) formed by the transplanted drNPC-O2 compared with the nontreated transplanted group, which was more prominent in caudal regions below the level of injury (1.66-fold; Fig. 9*B–D*). ILP/ISP co-treatment only moderately (but not significantly) increased inhibitory synapse formation by engrafted drNPC-O2 (Fig. 9*F–H*).

Next, we asked whether drNPC-O2-derived neurons could form synaptic connections with descending CST axons as a major supraspinal motor pathway innervating spinal cord interneurons and motoneurons (Karadimas et al., 2020). We anterogradely labeled the projecting CST axons in the spinal cord by injection of AAV8-mCherry viral particles into the sensorimotor cortex of SCI rats two weeks before their experimental end-point (Fig. 9*I*,*I'*). Co-immunohistochemical staining for synaptophysin and vGlut1 or GABAr showed drNPC-O2-derived neurons have the potential to form both excitatory (Fig. 9*J*,*J'*) and inhibitory (Fig. 9*K*,*K'*) synapses with AAV8-mCherry labeled CST terminals. Altogether, these findings suggest transplanted human drNPC-O2 can generate mature neurons with the ability to make excitatory and inhibitory synapses indicating their potential to integrate with the host damaged spinal neural network.

Transcriptomic analysis asserts the positive effects of LAR and PTPσ co-inhibition on the properties of transplanted human drNPC-O2 in the injured spinal cord

To better substantiate the properties of drNPC-O2-derived cells after transplantation in SCI and their response to ILP/ISP co-treatment, we preformed whole RNA-seq on the spinal cord of SCI rats at 14 weeks after transplantation. Reads were aligned to the human genome (hg19) using STAR package and differential expression analysis for rat versus human transcriptome was conducted with DeSeq2 package. These analyses successfully extracted human transcripts from the

←

(synaptophysin/vGlut1) and inhibitory (synaptophysin/GABAr) synapses with human drNPC-O2-derived neurons (WM: white matter, GM: gray matter). Values represent mean ± SEM, $^*p < 0.05$; nonparametric Student's *t* test, $N = 4$ animals. ns: non-significant.

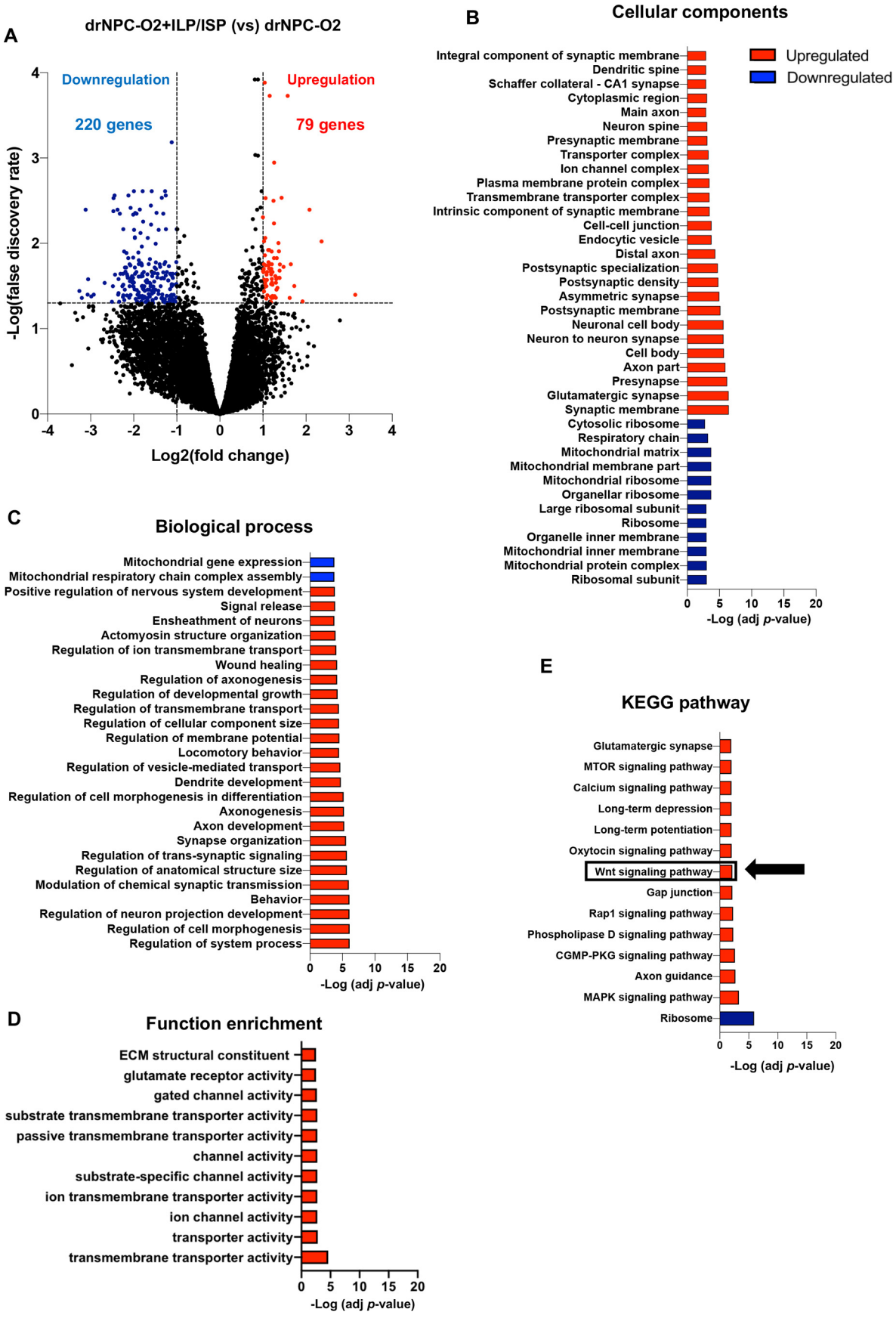

Figure 10. Transcriptomic analysis of human drNPC-O2 reveals significant increase in neuronal differentiation, maturation, and synaptic transmission by ILP/ISP treatment in the injured spinal cord. ***A***, Volcano plot illustrates differentially expressed genes at 14 weeks after transplantation (FDR $<$ 0.05, Benjamini–Hochberg, two-sided; fold change $>$ 2). ***B***, Gene Ontology analysis for cellular components using R language program identifies significantly upregulated and downregulated genes in transplanted drNPC-O2 after ILP/ISP co-treatment. These analyses showed

total RNA isolated from the injured rat spinal cord containing xenograft, indicating human RNA comprised ~20% of the total transcriptomics. We identified 299 genes (220 downregulated and 79 upregulated genes) that were differentially expressed in transplanted human cells in SCI rats that received co-ILP/ISP treatment compared with the vehicle treated group (false discovery rate (FDR) of adj-p value < 0.05; Fig. 10*A*). Co-ILP/ISP treatment promoted pathways associated with morphogenesis and cellular maturity of neurons including dendritic spine, cell body and axons (Fig. 10*B*). More importantly, ILP/ISP co-treatment enhanced genes associated with neuron-to-neuron synaptic connectivity, presynaptic and postsynaptic membrane density as well as integrated component of synaptic membrane confirming our immunohistological data that co-inhibition of LAR and PTPσ promotes excitatory synaptogenesis (Fig. 10*B*). In addition to cellular components, ILP/ISP co-administration promoted transcript expression of biological processes involved in neuronal functions including ion channel and transmembrane transporter activity, modulation of synaptic transmission and transduction at the molecular level (Fig. 10*C*,*D*). KEGG pathway analysis also showed increased synaptic transmission associated with glutaminergic synaptic activity, which verified our immunohistochemical analysis, as well as long-term potentiation and long-term depression indicating that ILP/ISP treatment may potentially improve synaptic plasticity of drNPC-O2 (Fig. 10*E*). Moreover, pathway analysis displayed upregulation in different cellular pathways such as mTOR and Wnt/β-catenin signaling pathways including Wnt11, Frizzled receptor, Wnt/β-catenin downstream transcription factor (TCF/LEF), and Rap1 signaling pathways (Fig. 10*D*). Among these upregulated pathways, Wnt/β-catenin is one of the regulatory pathways involved in neuronal differentiation of spinal cord NPCs (Li et al., 2018; Nguyen et al., 2018; Cui et al., 2019; Sun et al., 2020). Hence, we focused on this pathway to identify whether CSPG/LAR/PTPσ axis may regulate neuronal differentiation of drNPC-O2 by modulating Wnt/β-catenin pathway.

CSPGs inhibit neuronal differentiation of human drNPC-O2 by suppressing Wnt/β-catenin signaling pathway that can be reversed by co-blockage of LAR and PTPσ receptors

Wnt/β-catenin signaling pathway is known as a major regulator of spinal cord development, in particular, ventral spinal cord neuronal fate determination (Yu et al., 2008; Clements et al., 2009; Vanderhaeghen, 2009; Mulligan and Cheyette, 2012; Xing et al., 2018; Cui et al., 2019). First, we verified whether CSPGs inhibit neuronal differentiation of drNPC-O2 by suppressing Wnt/β-catenin signaling activity through LAR and PTPσ receptors. To address this question, we used our *in vitro* setting and plated drNPC-O2 onto laminin or laminin+CSPGs substrate. Then, we manipulated Wnt/β-catenin signaling in drNPC-O2 by CHIR99021 (pathway activator) or IWR01 (pathway inhibitor; Fig. 11*A*). These experiments showed activating Wnt/β-catenin pathway by CHIR99021 was able to significantly reverse CSPG inhibitory effects on neurogenesis of drNPC-O2 in a concentration dependent manner (2.35-fold increase on CSPGs 2.5 μg/ml and 5.08-fold increase on CSPGs 5 μg/ml), indicating CSPGs restrict neuronal differentiation via deactivation of Wnt/β-catenin (Fig. 11*A*,*B*). Concomitantly, CHIR99021 significantly attenuated astrocyte differentiation of drNPC-O2 on CSPGs (45.77% reduction on CSPGs 2.5 μg/ml and 33.42% reduction on CSPGs 5 μg/ml; Fig. 11*C*,*D*). In these experiments, Wnt activation had no effects on baseline neurogenesis of drNPC-O2 on laminin substrate. Conversely, suppressing Wnt/β-catenin by IWR01 significantly reduced neuronal differentiation (53.65% increase) while increased astrocyte differentiation (4.03-fold) of drNPC-O2 on control laminin substrate confirming the role of Wnt/β-catenin in neurogenic fate of drNPC-O2 (Fig. 11*A*–*D*).

To determine whether CSPGs inhibit Wnt/β-catenin pathway in drNPC-O2 through LAR and PTPσ receptors, we assessed the nuclear translocation of β-catenin, as an indicator of Wnt/β-catenin activity, under ILP/ISP co-treatment (Fig. 11*E*). Interestingly, blocking LAR and PTPσ receptors significantly enhanced β-catenin nuclear translocation on CSPGs (by 3.37-fold on CSPGs 2.5 μg/ml and by 4.25-fold CSPGs 5 μg/ml; Fig. 11*F*). Collectively, our findings suggest that CSPGs inhibit neurogenesis of drNPC-O2 by blocking Wnt/β-catenin singling pathway through LAR and PTPσ receptors, and ILP/ISP co-administration can therapeutically restore CSPGs-mediated suppression of neuronal differentiation by re-activating Wnt/β-catenin singling pathway.

ILP/ISP and drNPC-O2 transplantation synergistically improves recovery of locomotion and sensorimotor integration following SCI without altering pain sensation

We next evaluated whether the positive cellular and structural effects of combining a six-week ILP/ISP treatment regimen with drNPC-O2 grafts would facilitate long-term functional recovery after SCI. We performed longitudinal assessments of locomotion and thermal and mechanical sensitivity over a 15-week period after SCI. For assessing hindlimb locomotion, we used the widely accepted BBB motor rating scale weekly by two examiners blinded to the treatment groups. In these functional experiments, we included four SCI experimental groups to assess individual effects of ILP/ISP and drNPC-O2 treatments in addition to their combined effects. Our experimental groups included (1) SCI/vehicle (injury baseline); (2) SCI/ILP+ISP; (3) SCI/drNPC-O2; and (4) SCI/ILP/ISP+drNPC-O2. Our BBB assessments showed the vehicle SCI group that represents the injury baseline reached a plateau in BBB score on week 10 after injury and onwards with an average score of 10.72 ± 0.92 at the experimental endpoint on week 15 post-SCI (Fig. 12*A*). However, at the end point, BBB of animals that received drNPC-O2 alone or ILP/ISP alone were 11.72 ± 1.15 and 12.33 ± 1.49, respectively. Although these two groups had higher BBB scores compared with vehicle treated group, their recovery was not statistically significant (Fig. 12*A*). Interestingly, animals that received combination of drNPC-O2+ILP/ISP treatments reached an average BBB score of 13.29 ± 1.00 at 15 weeks post-SCI, which was significantly greater than the vehicle treated SCI group. Of note, drNPC-O2+ILP/ISP treated group did not reach a plateau in their BBB score by the experimental endpoint on week 15, suggesting that this combinatorial therapeutic strategy may result in further

←

that cellular components related to neurogenesis and synapse formation were upregulated by blocking LAR and PTPσ receptors. ***C***, Gene Ontology analysis for biological processes on human-exclusive transcripts indicated upregulation in biological processes related to neural regeneration and functional improvement with ILP/ISP treatment. ***D***, Gene Ontology analysis for functional enrichment of differentially expressed genes suggests blocking LAR and PTPσ receptors upregulates genes related to neuronal transmission and function. ***E***, KEGG pathway analysis of human-exclusive transcripts indicated that Wnt/β-catenin signaling pathway is upregulated by inhibiting LAR and PTPσ receptors. Fisher's exact test, FDR < 0.05, $N = 3$ animals per group.

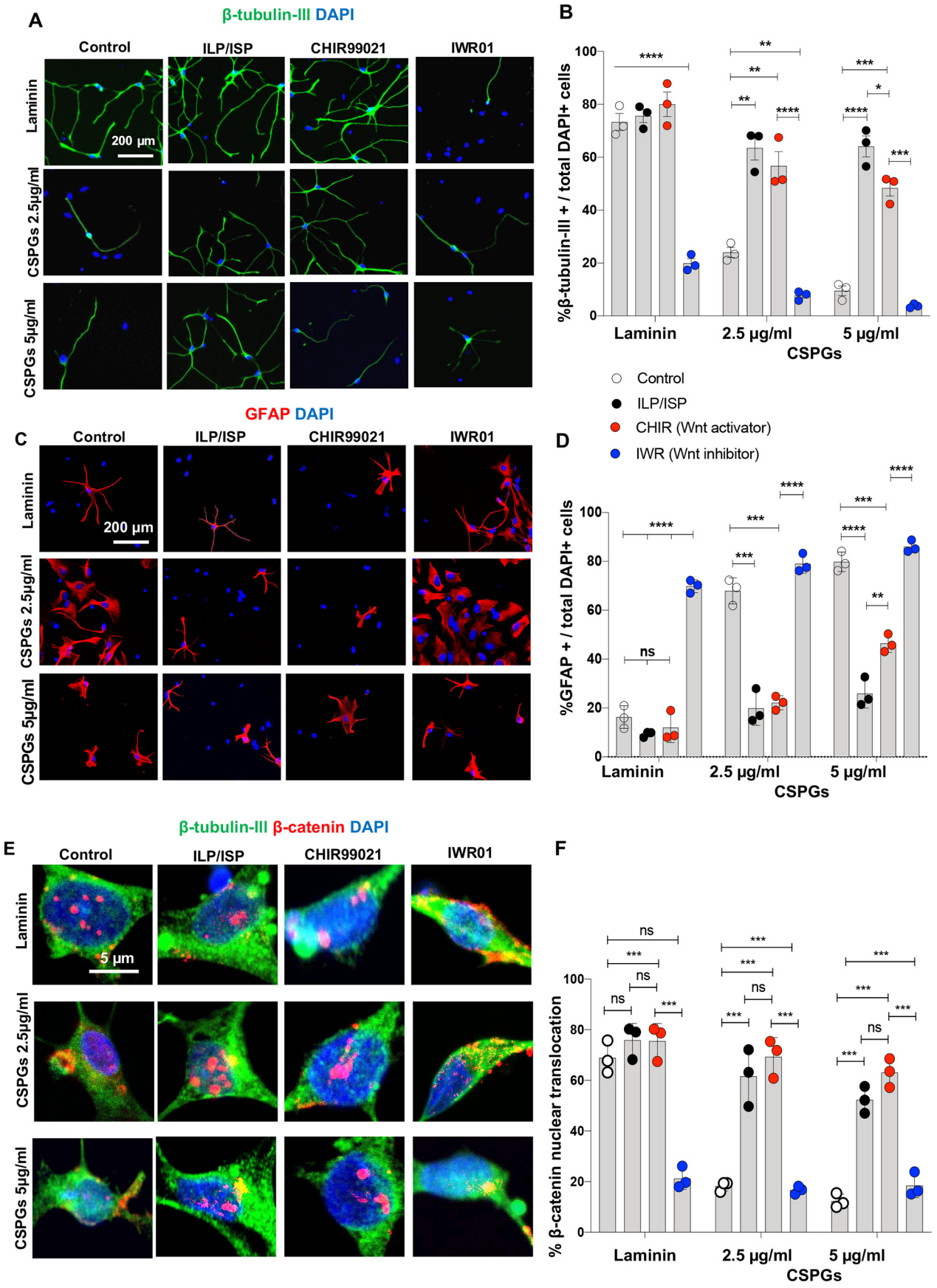

Figure 11. CSPGs inhibit neuronal differentiation of human drNPC-02 by suppressing Wnt/β-catenin pathway that can be reversed by co-blockage of LAR and PTPσ receptors *in vitro*. ***A***, ***B***, Role of Wnt/β-catenin pathway in neuronal differentiation of drNPC-02 on laminin and laminin+CSPGs was studied using Wnt-specific inhibitor (IWR01) and activator (CHRI99021). ***A***, Representative images of β-tubulin-III immunocytochemistry are depicted for differentiated drNPC-02 on laminin and/or CSPGs under ILP/ISP, CHIR99021, and IWR01 treatments. ***B***,

improvement in motor recovery beyond our 15-week studies. Future work is warranted to follow the functional outcome of this strategy over a much longer duration. Our heat-map analysis of BBB data showed that 41.6% of animals in drNPC-O2+ILP/ISP group had BBB score >14, which was significantly higher comparing to other groups with only 11.11–27.27% of the animals showed BBB score >14 (Fig. 12*B*). Of note, a BBB score of 14 and above indicates consistent plantar weight support and consistent forelimb-hindlimb coordination in SCI rats. Furthermore, we assessed sensorimotor integrity of SCI rats by grid walk analysis on an elevated horizontal ladder. At 13 and 15 weeks after injury, SCI animals in drNPC-O2 + ILP/ISP group exhibited significantly fewer foot falls per session (6.04 ± 2.92 and 4.38 ± 2.32, respectively) comparing to vehicle group (8.33 ± 2.28 and 6.85 ± 3.48; Fig. 12*C*). We also examined degree of pain sensitivity to thermal and mechanical stimuli in SCI rats at weeks 11, 13, and 15 postinjury using tail flick and von Frey tests, respectively (Fig. 12*D*,*E*). There was no significant difference in their pain response to thermal (Fig. 12*D*) and mechanical (Fig. 12*E*) stimuli across all SCI groups indicating these treatments did not affect pain response after SCI. Taken together, our findings indicate the synergistic benefits of combining drNPC-O2 grafts and co-inhibition of LAR and PTPσ receptors in improving locomotor recovery after SCI.

Discussion

Extensive degeneration of spinal cord neurons is a hallmark of traumatic SCI (Dietz and Fouad, 2014). Proper replenishment of spinal cord-specific neurons after injury is a complex process that involves timely activation of intrinsic and extrinsic mechanisms to support differentiation, maturation, and integration of new neurons within spinal cord circuits. Connectivity of these new neurons with their targets is particularly important to enable functional re-assembly of synapses (Dietz and Fouad, 2014; Fischer et al., 2020). Since neurons are generally susceptible to degeneration after SCI, regeneration of various neuronal subtypes including motoneurons and spinal cord-specific interneurons is required for proper re-construction of spinal networks. In neurodevelopment, NPCs acquire distinct genetic signature within the rostral and caudal CNS regions that results in generation of brain and spinal cord-specific neurons enabling formation of specialized local neural circuitry (Imai and Yoshida, 2018; Plant et al., 2018). Despite this developmental capacity, spontaneous neurogenesis is a rare phenotype of resident NPCs after SCI, as they primarily support gliogenesis (Barnabé-Heider et al., 2010; Stenudd et al., 2015). Replacement of damaged spinal cord neurons through transplantation of multipotent adult NPCs has been similarly challenging as astrogenesis is the predominant fate of engrafted NPCs after SCI (Hwang et al., 2019; Khazaei et al., 2020; Yang et al., 2021). Interestingly, when NPCs are isolated from the adult spinal cord and grown in culture, they show neurogenic potential (Mothe et al., 2005; Barnabé-Heider et al., 2010), indicating the presence of extrinsic regulatory mechanisms that actively impede their neuronal differentiation in the spinal cord.

In the present study, we have unraveled that injury-induced upregulation of CSPGs in the ECM of the injured spinal cord is a negative regulator of adult NPCs and an underlying mechanism that restricts neuronal differentiation in transplantation strategies. Targeting CSPGs receptors, LAR and PTPσ, using functional blocking peptides was sufficient to promote long-term survival of human drNPC-O2 and support their differentiation and maturation to motoneurons as well as V1 inhibitory and V3 excitatory interneurons, while reducing astrogenesis. Our direct *in vitro* studies showed that LAR and PTPσ receptors are both involved in mediating the inhibitory effects of CSPGs on human drNPC-O2, and their co-inhibition was essential to synergistically and significantly reverse CSPGs effects. Intriguingly, exposure to CSPGs suppressed multiple properties of human drNPC-O2 including their survival, growth, spreading, proliferation and neuronal differentiation, suggesting modulation of various intracellular cascades in NPCs. This is in fact in agreement with our previous *in vitro* studies on mouse-derived NPCs that identified CSPGs repress activation of Erk1/2 and Akt pathways while enhancing activation of Rho/ROCK pathway in NPCs (Dyck et al., 2015).

CSPGs also play critical roles in neural development and regulating NPC niches in the developing and normal adult brain in particular, where they are present abundantly and contribute to maintaining the pool of NPCs (Snow et al., 1991; Brittis et al., 1992; Sirko et al., 2007, 2010; Dyck and Karimi-Abdolrezaee, 2015). Intriguingly, CSPGs play a supportive role in proliferation and neurogenesis of NPCs in neurodevelopment (Kabos et al., 2004; Ida et al., 2006; Sirko et al., 2007, 2010), and degrading CSPGs results in impaired neurogenesis and brain development (Sirko et al., 2010). A recent study demonstrates that elevated levels of CSPGs promote neurogenesis in adult hippocampus (Yamada et al., 2018). Early studies also showed CSPGs are abundantly expressed in the developing mouse brain and promote attachment and neurite outgrowth of embryonic neurons (Faissner et al., 1994; Gates et al., 1996). Although the role of CSPGs in regulating spinal cord stem cell niche is yet to be investigated, these brain studies suggest beneficial effects of CSPGs on NPCs and neurogenesis during development and homeostasis, which is in contrast to the inhibitory effects of pathologic up-regulation of CSPGs on survival and neurogenesis of transplanted NPCs in our SCI studies. These differential effects may reflect several factors: (1) the pathologic, dysregulated levels of CSPGs in the injured spinal cord compared with their baseline expression in the brain under the developing and homeostasis conditions; (2) their differential effects on NPCs in the spinal cord verses brain regions; and/or (3) signaling through other receptors as CSPGs can also bind in lower affinity to Nogo receptors, NgR1 and NgR3 and influences integrin/laminin signaling (Dickendesher et al., 2012). Given the importance of CSPGs in both homeostasis and injury conditions, future studies are

←

Immunocytochemical quantification of drNPC-O2 showed that inhibiting Wnt/β-catenin signaling pathway by IWR01 blocked neurogenesis of drNPC-O2 on laminin control condition, suggesting the importance of this pathway for neuronal differentiation of drNPC-O2. CHIR99021 was also sufficient to restore the inhibitory effects of CSPGs on neuronal differentiation by activating Wnt/β-catenin signaling pathway. ***C***, Representative images of GFAP immunocytochemistry for assessing astrocyte differentiation of drNPC-O2 on laminin and/or CSPGs under ILP/ISP, CHIR99021, and IWR01 treatments. ***D***, Activation of Wnt/β-catenin by CHRI99021 decreases astrocyte differentiation of drNPC-O2 on CSPGs, while blocking Wnt/β-catenin signaling pathway by IWR01 increases astrogenesis on laminin. ***E***, Representative immunostaining images show expression of β-catenin and β-tubulin-III in drNPC-O2-derived neurons under various conditions. ***F***, Analysis of β-catenin nuclear translocation revealed that inhibiting LAR and PTPσ receptor by ILP/ISP can significantly enhance Wnt/β-catenin pathway activity in neurons exposed to CSPGs similar to treatment with CHRI99021. Values represent mean ± SEM, $^*p < 0.05$; multiple *t* test, $N = 3$ independent cultures. ns: non-significant.

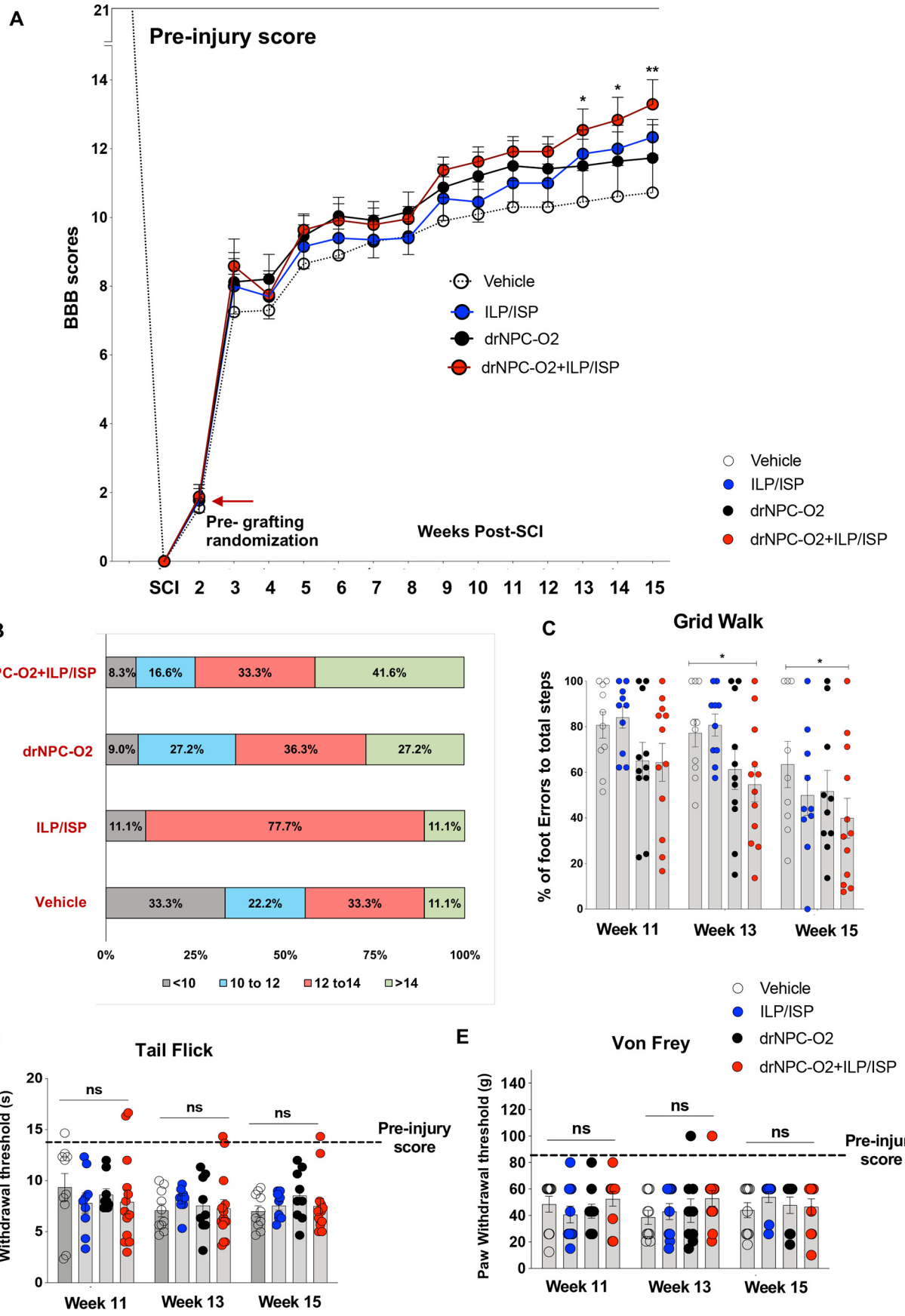

Figure 12. Transplantation of drNPC-O2 and ILP/ISP treatment synergistically improves motor recovery and sensorimotor integration after SCI. ***A–C***, Longitudinal assessment of locomotion was conducted for SCI animals in different groups by BBB open field and grid walking sensorimotor tests. ***A***, BBB assessment showed animals that received drNPC-O2 transplantation in combination with ILP/ISP treatment exhibited statistically significant improvement in their hindlimb locomotion compared with vehicle treated SCI rats. While rats that received drNPC-O2+ILP/ISP

required to understand how CSPGs regulate the activity of endogenous spinal cord NPCs under physiological and injury conditions.

Our *in vitro* and SCI studies showed CSPGs potently reduce survival of human drNPC-O2 that can be reversed by ILP/ISP co-treatment. Although our *in vitro* experiments confirmed CSPGs can directly affect NPC survival through activation of LAR and PTPσ, ILP/ISP treatment may also indirectly promote survival of engrafted NPCs in SCI by attenuating the proinflammatory role of CSPGs/LAR/PTPσ signaling. Our previous studies in rat SCI demonstrated that CSPGs potentiate a proinflammatory immune response in the injured spinal cord that is also mediated by LAR and PTPσ signaling (Dyck et al., 2018). Thus, the beneficial effects of ILP/ISP co-treatment on drNPC-O2 survival and transplant volume in the present study may be partly attributed to attenuating the proinflammatory function of CSPGs/LAR/PTPσ axis after SCI.

Inhibition of LAR and PTPσ promoted differentiation and maturation of human drNPC-O2 to ChAT motoneurons, V1 inhibitory and V3 excitatory interneurons. Importantly, targeting LAR and PTPσ further enhanced formation of inhibitory and excitatory synapses among human drNPC-O2-derived neurons which was correlated with improved recovery of locomotion and sensorimotor integration in SCI rats. These interneurons are important for functional recovery after SCI (Trawczynski et al., 2019; Lee et al., 2020) as V1 interneurons regulate locomotion speed as well as flexor and extensor alternation (Li et al., 2004; Gosgnach et al., 2006; Falgairolle and O'Donovan, 2019), and V3 interneurons play an important role in locomotion flexibility, left-right hindlimb coordination, balanced locomotor rhythm and initiating motor movement (Zhang et al., 2008; Chopek et al., 2018; Danner et al., 2019; Lin et al., 2019). Our data also suggest that drNPC-O2-derived neurons appears to form connections with the host projecting CST axons. However, further studies using specific trans-synaptic tracing approaches are required to confirm whether transplanted human drNPCs-O2-derived neurons make synaptic contact and receive input through the host descending CST axons.

Our global transcriptomic analysis of engrafted human drNPC-O2 in the injured spinal cord further confirmed that co-inhibition of LAR and PTPσ receptors promotes a program of gene expression in drNPC-O2 that can support neuronal differentiation, maturation, signal transmission, synaptic plasticity and behavioral improvement. Interestingly, our KEGG pathway analysis revealed higher expression of Wnt/β-catenin in SCI rats that received ILP/ISP treatment, suggesting LAR/PTPσ signaling represses this pathway in NPCs after SCI. Our parallel *in vitro* studies also verified that CSPGs inhibit neuronal maturation of human drNPC-O2 by inhibiting Wnt/β-catenin pathway, which can be rescued by blocking LAR/PTPσ signaling. Wnt/β-catenin signaling is known for its major role in the expansion, proliferation and differentiation of spinal cord progenitor pool in dorsal and ventral developing spinal cord (Ille et al., 2007; Yu et al., 2008; Joksimovic et al., 2012; Lambert et al., 2016; Xing et al., 2018; Cui et al., 2019). Evidence shows that Wnt/β-catenin regulates proliferation and cell cycle exit of spinal cord NPCs by modulating the expression of cyclin-dependent kinase (CdK) inhibitor (p57/kip2 and p27/kip1; David et al., 2010). Activation of Wnt/β-catenin also increases neuronal differentiation of mouse spinal cord NPCs *in vitro* through inhibition of GSK-3β (David et al., 2010). Intriguingly, upregulation of Wnt/β-catenin after SCI in zebrafish and lampreys has been associated with the remarkable capacity of these lower vertebrates in successful regeneration and recovery after SCI (Strand et al., 2016; Herman et al., 2018). Activation of Wnt/β-catenin is also critical for radial glial neurogenesis in zebrafish after SCI (Briona et al., 2015). In mammals, recent studies in a rat model of SCI demonstrate that activation of Wnt/β-catenin enhances neuronal differentiation of transplanted NPCs and functional improvement (Li et al., 2018, 2020). More relevant to the present study, transplantation of Wnt4-expressing rat-derived NPCs rescues neuronal differentiation of transplanted cells resulting in hindlimb functional recovery in rat SCI (Li et al., 2020). These findings collectively suggest the significance of highly-conserved Wnt/β-catenin pathway in neurogenesis and recovery following SCI and underscores the importance of our new findings that identifies CSPGs/LAR/PTPσ signaling as a negative regulator of Wnt/β-catenin in SCI that restrict NPC neurogenesis and neuronal maturation.

In conclusion, we provide the first evidence for the inhibitory role of CSPGs/LAR/PTPσ axis in regulating NPC neurogenesis and functional integrity of newborn neurons in cell replacement strategies for SCI. In addition to uncovering new SCI mechanisms, this work has developed a clinically feasible regenerative strategy with the potential to optimize the outcomes of current cellular therapies for SCI repair. Human directly reprogramed caudalized NPCs provide a relevant cell source with the potential to replace spinal cord-specific neurons in the injured spinal cord. This approach also obviates the risk factors associated with engineered viral vector expressing NPCs that are employed in other studies to enhance neuronal differentiation by production of various growth factors (Nori et al., 2018; Vonderwalde et al., 2020; Namestnikova et al., 2021). Importantly, human drNPC-O2 provide the opportunity for autologous sources of NPCs for SCI clinical trials as they are reprogramed from blood cells. Our strategy for targeting LAR and PTPσ with systemic administration of ILP/ISP also represents a feasible therapeutic approach for SCI. Thus, this work has identified a new combinatorial therapy for SCI with translational potential, while dissecting the role of an important endogenous pathway in NPC regulation after SCI.

←

also had higher average of BBB score compared with drNPC-O2 or ILP/ISP alone groups, the difference was not statistically significant (***B***) χ^2 analysis also revealed significantly greater proportion of recovered animals with consistent weight support and coordination with predominant rotated paw position (BBB > 14) in the group which received drNPC-O2 + ILP/ISP comparing with animals in other groups. ***C***, Sensorimotor examination with grid-walk test also indicated significantly lower percentage of foot errors in hindlimbs of rats that received drNPC-O2 + ILP/ISP treatments after SCI. Uninjured animals showed no foot error in grid-walking analysis. ***D***, Tail flick test revealed that SCI causes thermal hypersensitivity in injured animals compared with uninjured normal baseline level. However, tail flick assessment revealed no significant difference in thermal pain sensitivity among SCI groups. ***E***, Likewise, Von Frey test indicated that SCI results in mechanical hypersensitivity comparing to normal (baseline) animals. However, we found no significant difference in mechanical pain sensitivity after SCI across treatment groups as the result of drNPC-O2 transplantation and/or ILP/ISP co-treatment. Values represent mean ± SEM, *$p < 0.05$; two-way ANOVA repeated measures followed by Fisher's LSD *post hoc*, $N =$ 10–12 animals/group. ns: non-significant.

References

Ahuja CS, Mothe A, Khazaei M, Badhiwala JH, Gilbert EA, van der Kooy D, Morshead CM, Tator C, Fehlings MG (2020) The leading edge: emerging neuroprotective and neuroregenerative cell-based therapies for spinal cord injury. Stem Cells Transl Med 9:1509–1530.

Alilain WJ, Horn KP, Hu H, Dick TE, Silver J (2011) Functional regeneration of respiratory pathways after spinal cord injury. Nature 475:196–200.

Alizadeh A, Dyck SM, Kataria H, Shahriary GM, Nguyen DH, Santhosh KT, Karimi-Abdolrezaee S (2017) Neuregulin-1 positively modulates glial response and improves neurological recovery following traumatic spinal cord injury. Glia 65:1152–1175.

Alizadeh A, Santhosh KT, Kataria H, Gounni AS, Karimi-Abdolrezaee S (2018) Neuregulin-1 elicits a regulatory immune response following traumatic spinal cord injury. J Neuroinflammation 15:53.

Alizadeh A, Dyck SM, Karimi-Abdolrezaee S (2019) Traumatic spinal cord injury: an overview of pathophysiology, models and acute injury mechanisms. Front Neurol 10:282.

Andrews EM, Richards RJ, Yin FQ, Viapiano MS, Jakeman LB (2012) Alterations in chondroitin sulfate proteoglycan expression occur both at and far from the site of spinal contusion injury. Exp Neurol 235:174–187.

Assinck P, Duncan GJ, Hilton BJ, Plemel JR, Tetzlaff W (2017) Cell transplantation therapy for spinal cord injury. Nat Neurosci 20:637–647.

Barnabé-Heider F, Göritz C, Sabelström H, Takebayashi H, Pfrieger FW, Meletis K, Frisén J (2010) Origin of new glial cells in intact and injured adult spinal cord. Cell Stem Cell 7:470–482.

Barritt AW, Davies M, Marchand F, Hartley R, Grist J, Yip P, McMahon SB, Bradbury EJ (2006) Chondroitinase ABC promotes sprouting of intact and injured spinal systems after spinal cord injury. J Neurosci 26:10856–10867.

Basso DM, Beattie MS, Bresnahan JC (1995) A sensitive and reliable locomotor rating scale for open field testing in rats. J Neurotrauma 12:1–21.

Blankenberg D, Hillman-Jackson J (2014) Analysis of next-generation sequencing data using galaxy. Methods Mol Biol 1150:21–43.

Briona LK, Poulain FE, Mosimann C, Dorsky RI, City SL, Carolina S (2015) Wnt/β-catenin signaling is required for radial glial neurogenesis following spinal cord injury. Dev Biol 403:15–21.

Brittis PA, Canning DR, Silver J (1992) Chondroitin sulfate as a regulator of neuronal patterning in the retina. Science 255:733–736.

Ceto S, Sekiguchi KJ, Takashima Y, Nimmerjahn A, Tuszynski MH (2020) Neural stem cell grafts form extensive synaptic networks that integrate with host circuits after spinal cord injury. Cell Stem Cell 27:430–440.e5.

Cheng L, Sami A, Ghosh B, Urban MW, Heinsinger NM, Liang SS, Smith GM, Wright MC, Li S, Lepore AC (2021) LAR inhibitory peptide promotes recovery of diaphragm function and multiple forms of respiratory neural circuit plasticity after cervical spinal cord injury. Neurobiol Dis 147:105153.

Chopek JW, Nascimento F, Beato M, Brownstone RM, Zhang Y (2018) Subpopulations of spinal V3 interneurons form focal modules of layered premotor microcircuits. Cell Rep 25:146–156.e3.

Clements WK, Ong KG, Traver D (2009) Zebrafish wnt3 is expressed in developing neural tissue. Dev Dyn 238:1788–1795.

Cregg JM, DePaul MA, Filous AR, Lang BT, Tran A, Silver J (2014) Functional regeneration beyond the glial scar. Exp Neurol 253:197–207.

Cui Y, Yin Y, Xiao Z, Zhao Y, Chen B, Yang B, Xu B, Song H, Zou Y, Ma X, Dai J (2019) LncRNA Neat1 mediates miR-124-induced activation of Wnt/β-catenin signaling in spinal cord neural progenitor cells. Stem Cell Res Ther 10:400.

Curtis E, Martin JR, Gabel B, Sidhu N, Rzesiewicz TK, Mandeville R, Van Gorp S, Leerink M, Tadokoro T, Marsala S, Jamieson C, Marsala M, Ciacci JD (2018) A first-in-human, phase I study of neural stem cell transplantation for chronic spinal cord injury. Cell Stem Cell 22:941–950.e6.

Danner SM, Zhang H, Shevtsova NA, Borowska-Fielding J, Deska-Gauthier D, Rybak IA, Zhang Y (2019) Spinal V3 interneurons and left–right coordination in mammalian locomotion. Front Cell Neurosci 13:516.

David MD, Cantí C, Herreros J (2010) Wnt-3a and Wnt-3 differently stimulate proliferation and neurogenesis of spinal neural precursors and promote neurite outgrowth by canonical signaling. J Neurosci Res 88:3011–3023.

Deng LX, Hu J, Liu N, Wang X, Smith GM, Wen X, Xu XM (2011) GDNF modifies reactive astrogliosis allowing robust axonal regeneration through Schwann cell-seeded guidance channels after spinal cord injury. Exp Neurol 229:238–250.

Dickendesher TL, Baldwin KT, Mironova YA, Koriyama Y, Raiker SJ, Askew KL, Wood A, Geoffroy CG, Zheng B, Liepmann CD, Katagiri Y, Benowitz LI, Geller HM, Giger RJ (2012) NgR1 and NgR3 are receptors for chondroitin sulfate proteoglycans. Nat Neurosci 15:703–712.

Dietz V, Fouad K (2014) Restoration of sensorimotor functions after spinal cord injury. Brain 137:654–667.

Dyck SM, Karimi-Abdolrezaee S (2015) Chondroitin sulfate proteoglycans: key modulators in the developing and pathologic central nervous system. Exp Neurol 269:169–187.

Dyck SM, Alizadeh A, Santhosh KT, Proulx EH, Wu CL, Karimi-Abdolrezaee S (2015) Chondroitin sulfate proteoglycans negatively modulate spinal cord neural precursor cells by signaling through LAR and RPTPσ and modulation of the rho/ROCK pathway. Stem Cells 33:2550–2563.

Dyck S, Kataria H, Alizadeh A, Santhosh KT, Lang B, Silver J, Karimi-Abdolrezaee S (2018) Perturbing chondroitin sulfate proteoglycan signaling through LAR and PTPσ receptors promotes a beneficial inflammatory response following spinal cord injury. J Neuroinflammation 15:90.

Dyck S, Kataria H, Akbari-Kelachayeh K, Silver J, Karimi-Abdolrezaee S (2019) LAR and PTPσ receptors are negative regulators of oligodendrogenesis and oligodendrocyte integrity in spinal cord injury. Glia 67:125–145.

Eftekharpour E, Karimi-Abdolrezaee S, Wang J, El Beheiry H, Morshead C, Fehlings MG (2007) Myelination of congenitally dysmyelinated spinal cord axons by adult neural precursor cells results in formation of nodes of ranvier and improved axonal conduction. J Neurosci 27:3416–3428.

Faissner A, Clement A, Lochter A, Streit A, Mandl C, Schachner M (1994) Isolation of a neural chondroitin sulfate proteoglycan with neurite outgrowth promoting properties. J Cell Biol 126:783–799.

Falgairolle M, O'Donovan MJ (2019) V1 interneurons regulate the pattern and frequency of locomotor-like activity in the neonatal mouse spinal cord. PLoS Biol 17:e3000447.

Fan J, Saha S, Barker G, Heesom KJ, Ghali F, Jones AR, Matthews DA, Bessant C (2015) Galaxy integrated omics: web-based standards-compliant workflows for proteomics informed by transcriptomics. Mol Cell Proteomics 14:3087–3093.

Fischer I, Dulin JN, Lane MA (2020) Transplanting neural progenitor cells to restore connectivity after spinal cord injury. Nat Rev Neurosci 21:366–383.

Fisher D, Xing B, Dill J, Li H, Hoang HH, Zhao Z, Yang XL, Bachoo R, Cannon S, Longo FM, Sheng M, Silver J, Li S (2011) Leukocyte common antigen-related phosphatase is a functional receptor for chondroitin sulfate proteoglycan axon growth inhibitors. J Neurosci 31:14051–14066.

Galtrey CM, Asher RA, Nothias F, Fawcett JW (2007) Promoting plasticity in the spinal cord with chondroitinase improves functional recovery after peripheral nerve repair. Brain 130:926–939.

Gates MA, Fillmore H, Steindler DA (1996) Chondroitin sulfate proteoglycan and tenascin in the wounded adult mouse neostriatum in vitro: dopamine neuron attachment and process outgrowth. J Neurosci 16:8005–8018.

Gauthier MK, Kosciuczyk K, Tapley L, Karimi-Abdolrezaee S (2013) Dysregulation of the neuregulin-1-ErbB network modulates endogenous oligodendrocyte differentiation and preservation after spinal cord injury. Eur J Neurosci 38:2693–2715.

Ge SX, Son EW, Yao R (2018) iDEP: an integrated web application for differential expression and pathway analysis of RNA-Seq data. BMC Bioinformatics 19:534.

Gosgnach S, Lanuza GM, Butt SJB, Saueressig H, Zhang Y, Velasquez T, Riethmacher D, Callaway EM, Kiehn O, Goulding M (2006) V1 spinal neurons regulate the speed of vertebrate locomotor outputs. Nature 440:215–219.

Grüning BA, Fallmann J, Yusuf D, Will S, Erxleben A, Eggenhofer F, Houwaart T, Batut B, Videm P, Bagnacani A, Wolfien M, Lott SC, Hoogstrate Y, Hess WR, Wolkenhauer O, Hoffmann S, Akalin A, Ohler U, Stadler PF, Backofen R (2017) The RNA workbench: best practices for RNA and high-throughput sequencing bioinformatics in galaxy. Nucleic Acids Res 45:W560–W566.

Harris KM, Spacek J, Bell ME, Parker PH, Lindsey LF, Baden AD, Vogelstein JT, Burns R (2015) A resource from 3D electron microscopy of hippocampal neuropil for user training and tool development. Sci Data 2:150046.

Hart CG, Dyck SM, Kataria H, Alizadeh A, Nagakannan P, Thliveris JA, Eftekharpour E, Karimi-Abdolrezaee S (2020) Acute upregulation of bone morphogenetic protein-4 regulates endogenous cell response and promotes cell death in spinal cord injury. Exp Neurol 325:113163.

Hendaoui I, Tucker RP, Zingg D, Bichet S, Schittny J, Chiquet-Ehrismann R (2014) Tenascin-C is required for normal Wnt/β-catenin signaling in the whisker follicle stem cell niche. Matrix Biol 40:46–53.

Herman PE, Papatheodorou A, Bryant SA, Waterbury CKM, Herdy JR, Arcese AA, Buxbaum JD, Smith JJ, Morgan JR, Bloom O (2018) Highly conserved molecular pathways, including Wnt signaling, promote functional recovery from spinal cord injury in lampreys. Sci Rep 8:742.

Hussein RK, Mencio CP, Katagiri Y, Brake AM, Geller HM (2020) Role of chondroitin sulfation following spinal cord injury. Front Cell Neurosci 14:208.

Hwang K, Jung K, Kim IS, Kim M, Han J, Lim J, Shin JE, Jang JH, Park KI (2019) Glial cell line-derived neurotrophic factor-overexpressing human neural stem/progenitor cells enhance therapeutic efficiency in rat with traumatic spinal cord injury. Exp Neurobiol 28:679–696.

Iavarone E, Yi J, Shi Y, Zandt BJ, O'reilly C, Van Geit W, Rössert C, Markram H, Hill SL (2019) Experimentally-constrained biophysical models of tonic and burst firing modes in thalamocortical neurons. PLoS Comput Biol 15:e1006753.

Ida M, Shuo T, Hirano K, Tokita Y, Nakanishi K, Matsui F, Aono S, Fujita H, Fujiwara Y, Kaji T, Oohira A (2006) Identification and functions of chondroitin sulfate in the milieu of neural stem cells. J Biol Chem 281:5982–5991.

Ille F, Atanasoski S, Falk S, Ittner LM, Märki D, Büchmann-Møller S, Wurdak H, Suter U, Taketo MM, Sommer L (2007) Wnt/BMP signal integration regulates the balance between proliferation and differentiation of neuroepithelial cells in the dorsal spinal cord. Dev Biol 304:394–408.

Imai F, Yoshida Y (2018) Molecular mechanisms underlying monosynaptic sensory-motor circuit development in the spinal cord. Dev Dyn 247:581–587.

Ippolito DM, Eroglu C (2010) Quantifying synapses: an immunocytochemistry-based assay to quantify synapse number. J Vis Exp (45):2270.

Iwanami A, Kaneko S, Nakamura M, Kanemura Y, Mori H, Kobayashi S, Yamasaki M, Momoshima S, Ishii H, Ando K, Tanioka Y, Tamaoki N, Nomura T, Toyama Y, Okano H (2005) Transplantation of human neural stem cells for spinal cord injury in primates. J Neurosci Res 80:182–190.

Jin MC, Medress ZA, Azad TD, Doulames VM, Veeravagu A (2019) Stem cell therapies for acute spinal cord injury in humans: a review. Neurosurg Focus 46:E10.

Joksimovic M, Patel M, Taketo MM, Johnson R, Awatramani R (2012) Ectopic Wnt/beta-catenin signaling induces neurogenesis in the spinal cord and hindbrain floor plate. PLoS One 7:e30266.

Kabos P, Matundan H, Zandian M, Bertolotto C, Robinson ML, Davy BE, John SY, Krueger Jr RC (2004) Neural precursors express multiple chondroitin sulfate proteoglycans, including the lectican family. Biochem Biophys Res Commun 318:955–963.

Karadimas SK, Satkunendrarajah K, Laliberte AM, Ringuette D, Weisspapir I, Li L, Gosgnach S, Fehlings MG (2020) Sensory cortical control of movement. Nat Neurosci 23:75–84.

Karimi-Abdolrezaee S, Eftekharpour E, Wang J, Morshead CM, Fehlings MG (2006) Delayed transplantation of adult neural precursor cells promotes remyelination and functional neurological recovery after spinal cord injury. J Neurosci 26:3377–3389.

Karimi-Abdolrezaee S, Eftekharpour E, Wang J, Schut D, Fehlings MG (2010) Synergistic effects of transplanted adult neural stem/progenitor cells, chondroitinase, and growth factors promote functional repair and plasticity of the chronically injured spinal cord. J Neurosci 30:1657–1676.

Karimi-Abdolrezaee S, Schut D, Wang J, Fehlings MG (2012) Chondroitinase and growth factors enhance activation and Oligodendrocyte differentiation of endogenous neural precursor cells after spinal cord injury. PLoS One 7: e37589.

Kataria H, Alizadeh A, Shahriary GM, Saboktakin Rizi S, Henrie R, Santhosh KT, Thliveris JA, Karimi-Abdolrezaee S (2018) Neuregulin-1 promotes remyelination and fosters a pro-regenerative inflammatory response in focal demyelinating lesions of the spinal cord. Glia 66:538–561.

Khazaei M, Ahuja CS, Nakashima H, Nagoshi N, Li L, Wang J, Chio J, Badner A, Seligman D, Ichise A, Shibata S, Fehlings MG (2020) GDNF rescues the fate of neural progenitor grafts by attenuating Notch signals in the injured spinal cord in rodents. Sci Transl Med 12:eaau3538.

Kucukdereli H, Allen NJ, Lee AT, Feng A, Ozlu MI, Conatser LM, Chakraborty C, Workman G, Weaver M, Sage EH, Barres BA, Eroglu C (2011) Control of excitatory CNS synaptogenesis by astrocyte-secreted proteins hevin and SPARC. Proc Natl Acad Sci U S A 108:E440–E449.

Kumamaru H, Kadoya K, Adler AF, Takashima Y, Graham L, Coppola G, Tuszynski MH (2018) Generation and post-injury integration of human spinal cord neural stem cells. Nat Methods 15:723–731.

Lambert C, Cisternas P, Inestrosa NC (2016) Role of Wnt signaling in central nervous system injury. Mol Neurobiol 53:2297–2311.

Lang BT, Cregg JM, Depaul MA, Tran AP, Xu K, Dyck SM, Madalena KM, Brown BP, Weng YL, Li S, Karimi-Abdolrezaee S, Busch SA, Shen Y, Silver J (2015) Modulation of the proteoglycan receptor PTPσ promotes recovery after spinal cord injury. Nature 518:404–408.

Lee H, Lee HY, Lee BE, Gerovska D, Park SY, Zaehres H, Araúzo-Bravo MJ, Kim JI, Ha Y, Schöler HR, Kim JB (2020) Sequentially induced motor neurons from human fibroblasts facilitate locomotor recovery in a rodent spinal cord injury model. Elife 9:e52069.

Levi AD, Anderson KD, Okonkwo DO, Park P, Bryce TN, Kurpad SN, Aarabi B, Hsieh J, Gant K (2019) Clinical outcomes from a multi-center study of human neural stem cell transplantation in chronic cervical spinal cord injury. J Neurotrauma 36:891–902.

Li WC, Higashijima SI, Parry DM, Roberts A, Soffe SR (2004) Primitive roles for inhibitory interneurons in developing frog spinal cord. J Neurosci 24:5840–5848.

Li X, Fan C, Xiao Z, Zhao Y, Zhang H, Sun J, Zhuang Y, Wu X, Shi J, Chen Y, Dai J (2018) A collagen microchannel scaffold carrying paclitaxel-liposomes induces neuronal differentiation of neural stem cells through Wnt/β-catenin signaling for spinal cord injury repair. Biomaterials 183:114–127.

Li X, Peng Z, Long L, Tuo Y, Wang L, Zhao X, Le W, Wan Y (2020) Wnt4-modified NSC transplantation promotes functional recovery after spinal cord injury. FASEB J 34:82–94.

Lin S, Li Y, Lucas-Osma AM, Hari K, Stephens MJ, Singla R, Heckman CJ, Zhang Y, Fouad K, Fenrich KK, Bennett DJ (2019) Locomotor-related V3 interneurons initiate and coordinate muscles spasms after spinal cord injury. J Neurophysiol 121:1352–1367.

Liu K, Sun Y, Liu D, Ye S (2017) Inhibition of Wnt/β-catenin signaling by IWR1 induces expression of Foxd3 to promote mouse epiblast stem cell self-renewal. Biochem Biophys Res Commun 490:616–622.

Llamosas N, Arora V, Vij R, Kilinc M, Bijoch L, Rojas C, Reich A, Sridharan BP, Willems E, Piper DR, Scampavia L, Spicer TP, Miller CA, Lloyd Holder J, Rumbaugh G (2020) SYNGAP1 controls the maturation of dendrites, synaptic function, and network activity in developing human neurons. J Neurosci 40:7980–7994.

Markram H, et al. (2015) Reconstruction and simulation of neocortical microcircuitry. Cell 163:456–492.

Martins-Neves SR, Paiva-Oliveira DI, Fontes-Ribeiro C, Bovée JVMG, Cleton-Jansen AM, Gomes CMF (2018) IWR-1, a tankyrase inhibitor, attenuates Wnt/β-catenin signaling in cancer stem-like cells and inhibits in vivo the growth of a subcutaneous human osteosarcoma xenograft. Cancer Lett 414:1–15.

McKeon RJ, Schreiber RC, Rudge JS, Silver J (1991) Reduction of neurite outgrowth in a model of glial scarring following CNS injury is correlated with the expression of inhibitory molecules on reactive astrocytes. J Neurosci 11:3398–3411.

Mothe AJ, Kulbatski I, Van Bendegem RL, Lee L, Kobayashi E, Keating A, Tator CH (2005) Analysis of green fluorescent protein expression in transgenic rats for tracking transplanted neural stem/progenitor cells. J Histochem Cytochem 53:1215–1226.

Mukherjee N, Nandi S, Garg S, Ghosh S, Ghosh S, Samat R, Ghosh S (2020) Targeting chondroitin sulfate proteoglycans: an emerging therapeutic strategy to treat CNS injury. ACS Chem Neurosci 11:231–232.

Mulligan KA, Cheyette BNR (2012) Wnt signaling in vertebrate neural development and function. J Neuroimmune Pharmacol 7:774–787.

Namestnikova DD, Gubskiy IL, Revkova VA, Sukhinich KK, Melnikov PA, Gabashvili AN, Cherkashova EA, Vishnevskiy DA, Kurilo VV, Burunova VV, Semkina AS, Abakumov MA, Gubsky LV, Chekhonin VP, Ahlfors JE, Baklaushev VP, Yarygin KN (2021) Intra-arterial stem cell transplantation in experimental stroke in rats: real-time MR visualization of transplanted cells starting with their first pass through the brain with regard to the therapeutic action. Front Neurosci 15:641970.

Nguyen H, Kerimoglu C, Pirouz M, Pham L, Kiszka KA, Sokpor G, Sakib MS, Rosenbusch J, Teichmann U, Seong RH, Stoykova A, Fischer A, Staiger JF, Tuoc T (2018) Epigenetic regulation by BAF complexes limits

neural stem cell proliferation by suppressing Wnt signaling in late embryonic development. Stem Cell Reports 10:1734–1750.

Nori S, Okada Y, Nishimura S, Sasaki T, Itakura G, Kobayashi Y, Renault-Mihara F, Shimizu A, Koya I, Yoshida R, Kudoh J, Koike M, Uchiyama Y, Ikeda E, Toyama Y, Nakamura M, Okano H (2015) Long-term safety issues of iPSC-based cell therapy in a spinal cord injury model: oncogenic transformation with epithelial-mesenchymal transition. Stem Cell Reports 4:360–373.

Nori S, Khazaei M, Ahuja CS, Yokota K, Ahlfors JE, Liu Y, Wang J, Shibata S, Chio J, Hettiaratchi MH, Führmann T, Shoichet MS, Fehlings MG (2018) Human oligodendrogenic neural progenitor cells delivered with chondroitinase ABC facilitate functional repair of chronic spinal cord injury. Stem Cell Reports 11:1433–1448.

Plant GW, Weinrich JA, Kaltschmidt JA (2018) Sensory and descending motor circuitry during development and injury. Curr Opin Neurobiol 53:156–161.

Rosenzweig ES, Brock JH, Lu P, Kumamaru H, Salegio EA, Kadoya K, Weber JL, Liang JJ, Moseanko R, Hawbecker S, Huie JR, Havton LA, Nout-Lomas YS, Ferguson AR, Beattie MS, Bresnahan JC, Tuszynski MH (2018) Restorative effects of human neural stem cell grafts on the primate spinal cord. Nat Med 24:484–490.

Salewski RP, Mitchell RA, Li L, Shen C, Milekovskaia M, Nagy A, Fehlings MG (2015) Transplantation of induced pluripotent stem cell-derived neural stem cells mediate functional recovery following thoracic spinal cord injury through remyelination of axons. Stem Cells Transl Med 4:743–754.

Sankavaram SR, Hakim R, Covacu R, Frostell A, Neumann S, Svensson M, Brundin L (2019) Adult neural progenitor cells transplanted into spinal cord injury differentiate into oligodendrocytes, enhance myelination, and contribute to recovery. Stem Cell Reports 12:950–966.

Shao A, Tu S, Lu J, Zhang J (2019) Crosstalk between stem cell and spinal cord injury: pathophysiology and treatment strategies. Stem Cell Res Ther 10:238.

Sirko S, Von Holst A, Wizenmann A, Götz M, Faissner A (2007) Chondroitin sulfate glycosaminoglycans control proliferation, radial glia cell differentiation and neurogenesis in neural stem/progenitor cells. Development 134:2727–2738.

Sirko S, Akita K, Von Holst A, Faissner A (2010) Structural and functional analysis of chondroitin sulfate proteoglycans in the neural stem cell niche. Methods Enzymol 479:37–71.

Snow DM, Watanabe M, Letourneau PC, Silver J (1991) A chondroitin sulfate proteoglycan may influence the direction of retinal ganglion cell outgrowth. Development 113:1473–1485.

Söllner JF, Leparc G, Hildebrandt T, Klein H, Thomas L, Stupka E, Simon E (2017) An RNA-Seq atlas of gene expression in mouse and rat normal tissues. Sci Data 4:170185.

Stenudd M, Sabelström H, Frisén J (2015) Role of endogenous neural stem cells in spinal cord injury and repair. JAMA Neurol 72:235–237.

Strand NS, Hoi KK, Phan TMT, Ray CA, Berndt JD, Moon RT (2016) Wnt/β-catenin signaling promotes regeneration after adult zebrafish spinal cord injury. Biochem Biophys Res Commun 477:952–956.

Sun X, Peng X, Cao Y, Zhou Y, Sun Y (2020) ADNP promotes neural differentiation by modulating Wnt/β-catenin signaling. Nat Commun 11:2984.

Takahashi H, Craig AM (2013) Protein tyrosine phosphatases PTPδ, PTPσ, and LAR: presynaptic hubs for synapse organization. Trends Neurosci 36:522–534.

Trawczynski M, Liu G, David BT, Fessler RG (2019) Restoring motor neurons in spinal cord injury with induced pluripotent stem cells. Front Cell Neurosci 13:369.

Vanderhaeghen P (2009) Wnts blow on NeuroD1 to promote adult neuron production and diversity. Nat Neurosci 12:1079–1081.

Vonderwalde I, Azimi A, Rolvink G, Ahlfors JE, Shoichet MS, Morshead CM (2020) Transplantation of directly reprogrammed human neural precursor cells following stroke promotes synaptogenesis and functional recovery. Transl Stroke Res 11:93–107.

Wu Y, Liu F, Liu Y, Liu X, Ai Z, Guo Z, Zhang Y (2015) GSK3 inhibitors CHIR99021 and 6-bromoindirubin-3′-oxime inhibit microRNA maturation in mouse embryonic stem cells. Sci Rep 5:8666.

Xie Y, Massa SM, Ensslen-Craig SE, Major DL, Yang T, Tisi MA, Derevyanny VD, Runge WO, Mehta BP, Moore LA, Brady-Kalnay SM, Longo FM (2006) Protein-tyrosine phosphatase (PTP) wedge domain peptides: a novel approach for inhibition of PTP function and augmentation of protein-tyrosine kinase function. J Biol Chem 281:16482–16492.

Xing L, Anbarchian T, Tsai JM, Plant GW, Nusse R (2018) Wnt/β-catenin signaling regulates ependymal cell development and adult homeostasis. Proc Natl Acad Sci U S A 115:E5954–E5962.

Yamada J, Nadanaka S, Kitagawa H, Takeuchi K, Jinno S (2018) Increased synthesis of chondroitin sulfate proteoglycan promotes adult hippocampal neurogenesis in response to enriched environment. J Neurosci 38:8496–8513.

Yang Y, Fan Y, Zhang H, Zhang Q, Zhao Y, Xiao Z, Liu W, Chen B, Gao L, Sun Z, Xue X, Shu M, Dai J (2021) Small molecules combined with collagen hydrogel direct neurogenesis and migration of neural stem cells after spinal cord injury. Biomaterials 269:120479.

Yu C, Xia K, Gong Z, Ying L, Shu J, Zhang F, Chen Q, Li F, Liang C (2019) The application of neural stem/progenitor cells for regenerative therapy of spinal cord injury. Curr Stem Cell Res Ther 14:495–503.

Yu W, McDonnell K, Taketo MM, Bai CB (2008) Wnt signaling determines ventral spinal cord cell fates in a time-dependent manner. Development 135:3687–3696.

Zhang N, Wei P, Gong A, Chiu WT, Lee HT, Colman H, Huang H, Xue J, Liu M, Wang Y, Sawaya R, Xie K, Yung WKA, Medema RH, He X, Huang S (2011) FoxM1 promotes β-catenin nuclear localization and controls Wnt target-gene expression and glioma tumorigenesis. Cancer Cell 20:427–442.

Zhang Y, Narayan S, Geiman E, Lanuza GM, Velasquez T, Shanks B, Akay T, Dyck J, Pearson K, Gosgnach S, Fan CM, Goulding M (2008) V3 spinal neurons establish a robust and balanced locomotor rhythm during walking. Neuron 60:84–96.

Zholudeva LV, Lane MA (2019) Transplanting cells for spinal cord repair: who, what, when, where and why? Cell Transplant 28:388–399.

Zhou X, Wahane S, Friedl MS, Kluge M, Friedel CC, Avrampou K, Zachariou V, Guo L, Zhang B, He X, Friedel RH, Zou H (2020) Microglia and macrophages promote corralling, wound compaction and recovery after spinal cord injury via Plexin-B2. Nat Neurosci 23:337–350.